Range Anxiety

Panle Jia Barwick Shanjun Li Tianli Xia *

November 6, 2025

PRELIMINARY: NOT FOR DISTRIBUTION

Abstract

Range anxiety, the fear of depleting battery before reaching a charging station, is often cited as a major barrier to electric vehicle (EV) adoption, yet there has been limited formal economic analysis to quantify its importance and understand the policy implications. We develop a continuous-time dynamic model of EV usage and charging decisions to quantify range anxiety as the utility loss from feasible yet unrealized trips due to perceived range constraints. Using high-frequency data of 188,000 EV trips and 30,000 charging events among 8,000 EVs in Shanghai, we recover model parameters governing consumer driving and charging decisions. The estimates imply that, across EV models with varying driving ranges, average range anxiety was about $1,900 in 2021 but declined to $1,200 in 2024, driven by improvements in charging infrastructure and, especially, increases in driving range. Policy simulations underscore the importance of coordinating investments in battery capacity and charging infrastructure to address range anxiety. Relative to socially optimal levels, Shanghai's EV market has under-invested in driving range while over-investing in charging infrastructure.

Keywords: Electric vehicles, range anxiety, charging infrastructure, dynamic model

JEL Classification Codes: L91, R13, R21

*Barwick: Department of Economics, UW-Madison, NBER, and CEPR, pbarwick@wisc.edu. Li: Doerr School of Sustainability and FSI, Stanford University, and NBER, shanli@stanford.edu. Xia: Simon Business School, University of Rochester, tianli.xia@rochester.edu. We thank seminar and conference participants at Rochester, UCSC, and PKU-HSBC for their helpful comments. We thank Xiufang Cao for excellent research assistance.

1 Introduction

The transportation sector accounts for about one-third of the global carbon emissions, making its electrification with a clean electricity grid a key strategy for decarbonization. Since being introduced into the mass market in 2011, global passenger EV sales have grown rapidly, reaching 17.1 million units, or 20% of new passenger vehicle sales, by 2024.[1] Market penetration, however, varies widely: EVs accounted for 40% of new vehicle sales in China, 28% in Europe, 11% in the United States, and just 5% in the rest of the world. Even within countries or regions, adoption is highly uneven.[2] Understanding the barriers to EV adoption and identifying solutions to address them is critical for the next phase of EV diffusion.

Consumer surveys and industry reports regularly identify range anxiety as one of the most significant barriers to EV adoption (Wardlaw, 2020; Chokshi et al., 2021; Klier and Rubenstein, 2022; Rainieri et al., 2023; Bloomberg Intelligence, 2024). Range anxiety refers to the fear of depleting the battery before reaching a charging station, stemming from the combination of limited driving range and inadequate charging infrastructure.[3] Despite its widely recognized importance, there is limited economic analysis of range anxiety or cost-effective strategies to mitigate it. To address this gap in the literature, we develop a micro-foundation of range anxiety using a continuous-time dynamic model of consumer driving and charging decisions. Based on estimated model parameters, we conduct policy simulations to evaluate the relative cost-effectiveness of investing in battery technologies and expanding charging infrastructure.

In the model, trip demands of varying distances arrive exogenously, and EV drivers decide whether to undertake a trip or initiate charging based on their remaining battery range, the convenience of the charging network, and charging prices. We define range anxiety as the utility loss from forgone trips, arising from the driver's perceived risk of having insufficient battery range to reach either the destination or a charging station. Our empirical analysis leverages a unique, granular, and high-frequency dataset on EV driving and charging behavior. It records the location and remaining range of 8,000 EVs at 5-second intervals, along with detailed information on charging, such as station location, price, charging duration, and quantity. The data contains about 188,000 trips and 30,000 charging events across four weeks

[1] EVs include both battery electric vehicles (BEVs) and plug-in hybrid electric vehicles (PHEVs).

[2] Within Europe, EVs accounted for nearly 90% of new vehicle sales in Norway, compared to less than 20% in Germany. In the U.S., EVs made up about 26% of new car registrations in California in 2024, but less than 7% in Texas.

[3] Early EV models typically offered only 100–200 miles per charge, well below the 300–400 miles that gasoline vehicles can travel on a full tank. In 2015, there were about 12,000 public EV charging stations in the U.S., compared to nearly 150,000 gasoline stations. By 2025, the number of public charging stations had grown to nearly 70,000.

each in 2021 and 2024. Using these rich data, we recover the model parameters to quantify the significance of range anxiety and conduct policy simulations.

We begin by documenting five key patterns in the data. First, the charging probability, defined as the share of charging events among both driving and charging events, is higher when the remaining range (i.e., state of charge) is low. This is intuitive, as a limited remaining range both constrains the ability to take trips and increases the need to recharge. Second, charging probability rises with charging access, especially at low remaining ranges, reflecting the reduced hassle cost when more stations are nearby. Third, charging probability falls with charging price, again most strongly when the remaining range is low. By contrast, when the remaining range is high, charging probability is unresponsive to either charging access or charging price. Fourth, if trips arrive independently of the remaining range, then drivers forgo over 60% of trips that would reduce their remaining range below 50 km and about 20% of trips that would leave them below 100 km. The fraction of feasible yet forgone trips declines as the remaining range increases. These patterns of forgone trips provide direct evidence of range anxiety. Fifth, among drivers with access to home chargers, the probability of charging at public stations is much flatter with respect to the remaining range, highlighting behavioral differences between those with and without home charging access.

We then estimate a continuous-time dynamic model to recover the structural parameters governing driving and charging decisions. We incorporate rich heterogeneity and a number of state variables: consumers are characterized by the full driving range of their EV (e.g., 250km vs. 400km), the charging network structure (2021 vs. 2024), and whether they have access to a home charger. The set of state variables for a driver at any given point in time includes the remaining range of his vehicle, attributes of his current location (number of local charging stations, local charging price, amenities, home vs. away from home), and whether at a peak hour. The estimates suggest that the probability of charging decreases with remaining range and charging prices, but increases with better charging access and rises for vehicles with longer driving ranges. In contrast, the probability of driving rises with remaining range but drops sharply if taking a trip reduces the remaining range below 50 or 100 km, or if the trip ends in areas with sparse or costly charging options. Finally, the estimated price elasticity of charging demand at fast public stations is -0.98 for drivers without home charging and -0.28 for those with home charging. The lower elasticity among drivers with home charging likely reflects their infrequent use of public stations.

Using the estimated parameters, we find that the willingness to pay (WTP) for improvements in driving range and charging access is substantial, especially among drivers without

home charging. In 2018, the average driving range of the existing EV stock was 318km, and there were 100 fast-charging stations in the city. By 2024, the average range increased to 383km, while the number of fast-charging stations surged to 2,268 (with a total of 40,000 fast chargers). For drivers without home chargers, the estimated WTP for these improvements is ¥62,000 (approximately $8,600), compared with ¥18,000 (or $2,500) for those with home chargers. The WTP exhibits diminishing returns for both driving range and charging access. Moreover, the two attributes are substitutes: the combined WTP from improving both is smaller than the sum of their individual effects.

We next quantify range anxiety by monetizing the utility loss from feasible but unrealized trips due to fear of getting stranded on the road. The average range anxiety across vehicles with different ranges was $2,550 in 2018, falling to $1,900 in 2021 and $1,200 in 2024. This decline reflects both the expansion of the charging network and, especially, improvements in driving range. Overall, the reduction in range anxiety accounts for over 50% of WTP for improved driving range and charging access among drivers without home chargers, and roughly 15% among those with home charging.

We use simulations to evaluate two common strategies for alleviating range anxiety: expanding charging infrastructure vs. increasing driving range. The socially optimal level of each is determined by maximizing the aggregate welfare, defined as consumer surplus net of the costs of improving range (via larger battery capacity) and charging access (through denser station networks). Our results reveal that the actual levels of charging access and driving range in Shanghai's EV market deviate substantially from the social optimum. Between 2018 and 2024, driving ranges consistently fell short of optimal levels. Charging infrastructure, in contrast, was insufficient in 2018 and 2021 but expanded so rapidly that by 2024 the number of stations was roughly double the social optimum. These results highlight the need to better coordinate investments in charging networks and battery capacity, especially since both are often supported by government policies such as subsidies.

Our paper contributes to four strands of literature. First, it extends the extensive work on consumer demand for EVs. Prior studies have primarily examined barriers to EV adoption—such as high upfront purchase costs, limited access to charging infrastructure, and the role of government policies in addressing these challenges (Springel, 2021a; Rapson and Muehlegger, 2023). A key finding in this literature is the importance of indirect network effects (the "chicken-and-egg" problem), whereby charging infrastructure investment and EV adoption reinforce each other through positive spillovers (Li et al., 2017; Li, 2023; Springel, 2021b; Jacqz and Johnston, 2024; Wang, 2024). While range anxiety is often invoked as an implicit mech-

anism linking charging access to EV adoption, it has not, to our knowledge, been formally defined. Qin and Scott (2023) examines how vehicle driving range interacts with fuel prices to affect EV demand. In contrast, our paper offers a micro-foundation for range anxiety through a continuous-time dynamic model and quantifies it directly using detailed data on driving and charging behavior.

Second, our paper contributes to the emerging literature on EV charging. A central question in this literature is how charging behavior responds to prices across different settings, including home, workplace, and public stations. Field experiments document substantial variation in price elasticities across contexts (Garg et al., 2024; La Nauze et al., 2024; Bernard et al., 2025; Bailey et al., 2025).[4] Relying on highly disaggregated data, other studies infer EV usage from household electricity consumption in California (Burlig et al., 2021), estimate the time cost of fueling gasoline vehicles among drivers in Michigan and use this estimate to benchmark the cost of charging (Dorsey et al., 2025), and examine the impact of charging on the electricity grid in Germany (Heid et al., 2024). Our paper extends this literature by examining how driving and charging respond to both charging prices and charging access, within a unified framework applied to highly granular observational data. Our structural estimates indicate a price elasticity of –1 for public charging. Notably, EV drivers with home charging exhibit a stronger response to price changes at home than to prices at public stations.

Third, our study contributes to the literature on policy design aimed at promoting EV adoption and infrastructure investment. We quantify the interaction between driving range and charging access through a micro-founded model of EV driving and charging decisions. Zhou and Li (2018) highlight the critical role of indirect network effects in EV diffusion and argue that government intervention may be necessary to coordinate consumer adoption and infrastructure development. Barwick et al. (2024) and Remmy (2025) examine automakers' incentives in supplying product attributes such as driving range, showing that market power and network effects can lead to socially suboptimal outcomes. Relatedly, Arkolakis et al. (2025) and Barwick et al. (2025) develop models to characterize optimal charging networks that account for road network and driving patterns. Complementing these studies, our analysis demonstrates that the combination of limited driving range (supplied by automakers) and sparse charging access (provided by station investors) is the fundamental source of range anxiety, and that this interaction jointly determines the socially optimal levels of vehicle

[4]For example, interventions on charging prices yield elasticity estimates of –0.4 for workplace charging at UCSD (Garg et al., 2024), –0.44 for home charging among Tesla owners in Australia (La Nauze et al., 2024), and –1.6 for home charging in Calgary (Bailey et al., 2025). A UK national intervention at public charging stations finds price elasticities of -2 to -2.9 (Bernard et al., 2025), with considerable heterogeneity.

range and charging network size.

Finally, our paper contributes to the literature on public-private interactions. Li and Springel (2025) study the relationship between public and private charging stations in the U.S. Cabral et al. (2025) examines the substitutability and complementarity between public and private R&D. Our policy simulations underscore the importance of coordinating policy instruments such as subsidies that target different market participants, echoing the insight from Liu (2025) on the value of a coordinated policy mix in the EV sector.

The remainder of the paper proceeds as follows. Section 2 describes the data and discusses key data patterns. Section 3 presents the empirical model and estimation strategy. Section 4 discusses the estimation results. Section 5 conducts policy simulations. Section 6 concludes.

2 Data Description

Our analysis draws on data from Shanghai, a city with 24.9 million residents and 4.15 million households. By the end of 2024, the city had 5.1 million registered passenger vehicles, including 1.51 million electric vehicles (EVs), the largest EV stock of any single city in the world. In 2024 alone, 278,000 new EVs were sold in Shanghai, accounting for 45% of all new passenger vehicle sales, a share that slightly exceeded the national average of 40%.[5]

Our main dataset consists of eight weekly cross-sections of detailed EV usage and driving records, with four weeks drawn from 2021 and four from 2024. The four weeks fall in January, March, August, and October and capture seasonal variations across the year. Each cross-section contains data on 1,100 battery EVs, randomly sampled from the active EV fleet in Shanghai, with complete information on all trips and charging events during the week. Trip records are based on GPS tracking and include driving location and distance, while charging records provide the state of charge (SOC, i.e., remaining battery capacity measured in percentage from 0% to 100%), charging duration, and price. There are a total of 188,000 trips and 30,000 charging events in our sample. Table A1 reports summary statistics.

Our second dataset, obtained from the Shanghai Electric Technology Center, covers all commercial fast-charging stations in Shanghai from 2020–2024, including each station's location, posted prices, and hourly usage. Merging this with the trip-level records allows us to measure the density of nearby fast-charging options and the price menu available at alternative stations for every trip in the primary dataset.

[5]Battery electric vehicles (BEVs) made up 71% of the EV stock and 89% of all new EV sales in Shanghai in 2024. Plug-in hybrid (PHEVs) accounted for the rest.

Our third dataset, from the Shanghai Municipal Government, reports time-of-use electricity tariffs for both commercial fast-charging facilities and home charging. Appendix Figure A8 plots the hourly tariffs by season. Peak-load schedules are similar across seasons, but summer and winter have four pricing tiers, whereas spring and autumn use three.

Shanghai experienced a drastic expansion of its charging network. The total number of fast chargers increased from 780 in January 2020 to 34,020 in December 2024, about a 44-fold expansion, with roughly 15 chargers per station on average (Figure 1). Panel (b) maps charging access across the city, measured by the inverse distance-squared weighted sum of charging stations. For example, A value of 12 corresponds to 12 charging stations within 1km or 3 charging stations within 0.5 km. In 2021, only the central districts with the highest population density had charging access above 12; by 2024, most urban areas exceeded this threshold. The average charging access was 2.08 in 2021 and 2.84 in 2024.

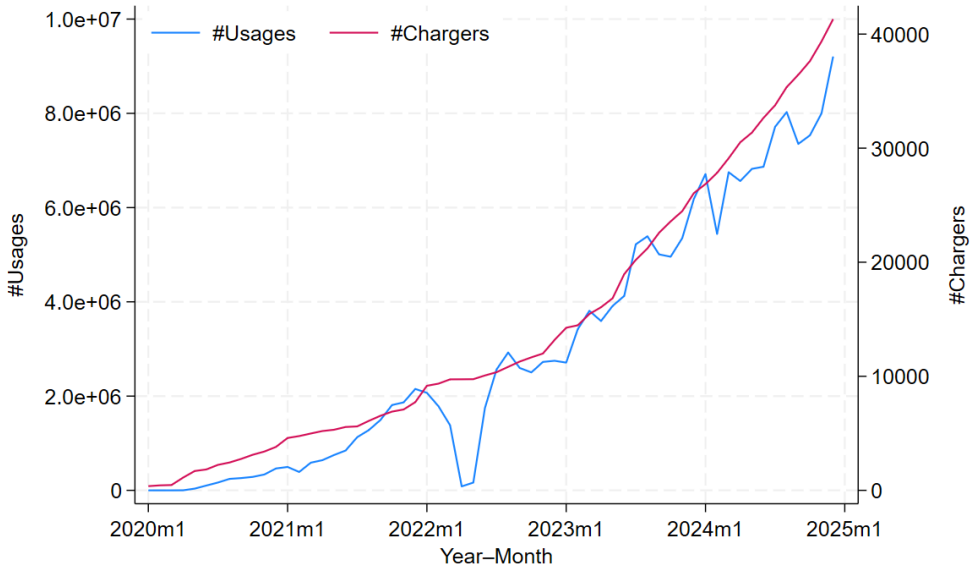
The average driving range of the existing EV stock in the main sample increased from 281 km in winter 2021 (January) to 331 km in winter 2024, as newer models tend to offer longer ranges (Figure 2, Panel (a)). Weekly usage also rose: the average number of trips per EV grew by 25%, from 20 in winter 2021 to 25 in winter 2024, while the corresponding weekly driving distance increased by 36%, from 335 km to 457 km (Figure 2, Panels (b)-(c)). Patterns are similar in the other seasons, with trip counts and driving distance increasing across the board from 2021 to 2024.

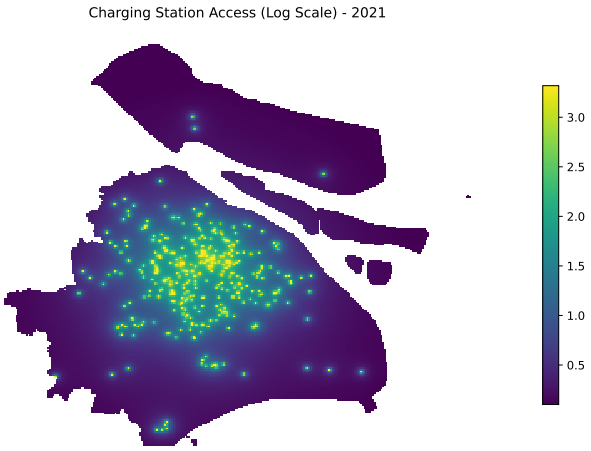
The expansion of the charging network also helps explain the sharp decline in reliance on slow charging. The share of drivers who exclusively used slow charging fell from 76.9% to 53.6% from 2021 to 2024 (a 30% drop), likely reflecting improved availability and reliability of fast-charging infrastructure. Consistent with this, the average weekly frequency of fast-charging per driver more than doubled from 0.7 in winter 2021 to 1.5 in winter 2024 (Figure 2, Panel (e)). Moreover, the average state of charge (remaining battery level) at the start of fast-charging sessions increased from 36% to 40%, suggesting that drivers are charging more proactively rather than waiting until the battery is close to depletion (Figure 2, Panel (g)).

Appendix Figure A1 plots the locations and frequency of charging events for fast and slow charging stations, separately, using the primary data source on charging trips. The data patterns align well with the location and usage reported in the data on all charging stations, verifying the representativeness of the trip sample.

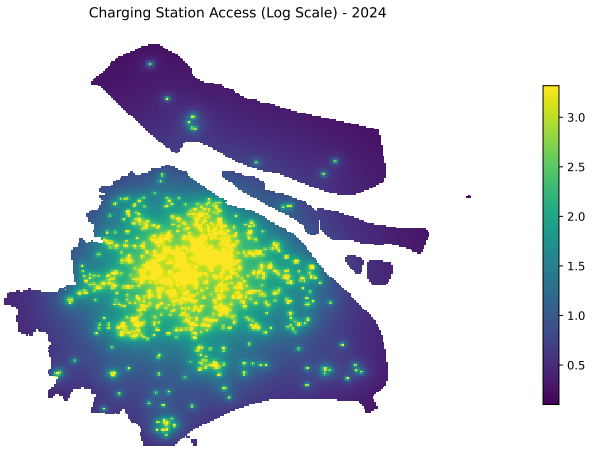
Overall, the data reveal a clear shift toward more frequent use of EVs and longer driving ranges, driven by improvements in vehicle performance and the rapid expansion of fast-charging infrastructure. Together, these developments signal a broader maturation of the EV

Figure 1: Numbers and Usage of Fast-Chargers





(a) Charging Access (2021)



(b) Charging Access (2024)

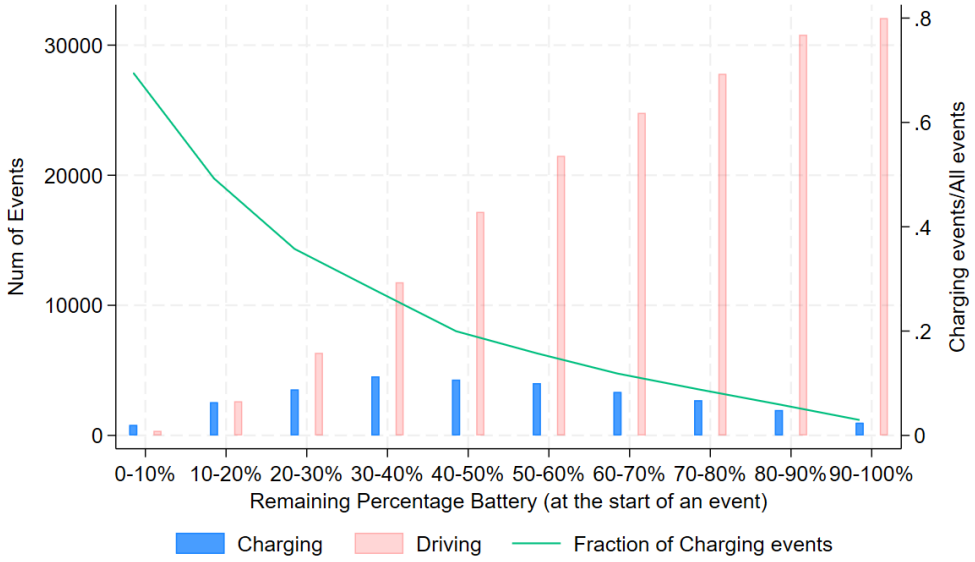
Note: The top figure shows the number of fast-charging chargers and their usage (number of charging events) in Shanghai. There are on average 15 chargers per station. Bottom Figures (a) and (b) report the log(charging access) of each location measured in 2021 and 2024. Charging access for location i is defined as the sum of the inverse squared distance to fast charging stations i. ($CA_i = \sum_j \frac{1}{dist_{ij}^2}$).

ecosystem between 2021 and 2024.

2.1 Descriptive Patterns

Our rich data on driving and charging trips reveal several interesting patterns. First, Figure 3 provides clear evidence that charging behavior is strongly influenced by the remaining battery level. Charging events (blue bars) are most likely to occur when the state of charge (SOC) is between 30% and 50%, and decline as SOC increases. In contrast, driving events (pink bars) are much more likely when SOC is high, with more than 80% of trips occurring when the battery level exceeds $> 50\%$. The green line represents the fraction of charging events among all events. It falls steadily with SOC, from about 70% when the remaining battery is below 10% to less than 10% when remaining battery exceeds 80% of full capacity.

Figure 3: Number of Events Events Given Remaining Battery



Second, charging behavior depends on charging convenience and price. To illustrate this, we group trip-level observations by the number of stations within 1 km (from 1 to 15 stations; Figure 4(a)) and plot a binned scatterplot of the charging probability (the ratio of charging trips to all trips) against this count. We do so separately for trips starting with SOC$<$40% and SOC $\geq$ 40%. We then overlay a smoothed quadratic trend line to highlight the overall patterns. Figure 4(b) repeats the analysis and plots the charging probability against the price at the nearest charging station.

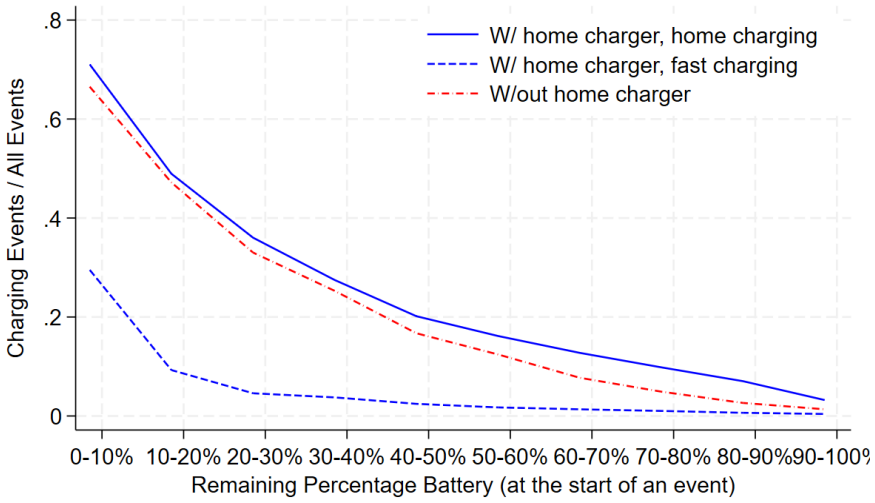
As shown in Figure 4, drivers' charging decisions vary with network size, with stronger

responses when the battery level is low (SOC<40%). The probability of initiating a charging trip rises sharply with the number of nearby stations for low-SOC trips, consistent with greater local station availability lowering search and hassle costs and thereby encouraging charging. In contrast, the relationship is much flatter for trips with SOC $>$ 40%, when drivers are less constrained and can delay charging or travel farther. Analogous patterns hold for prices: charging events are more likely to occur when prices are low, and drivers with low SOC are more responsive to price differences.

Third, there are more unrealized trips at low SOC, consistent with range anxiety. If the arrival rate of trips with different distances arrive orthogonally to SOC, then the number of trips per hour (the hazard rate) should be relatively flat across the remaining battery. Figure A3 shows that this is indeed the case when the remaining battery is relatively abundant. For example, the hazard rate is about 0.12 for trips shorter than 50 km and 0.05 for trips between 50 and 100 km. However, there is a clear dent in the hazard rate when the remaining range is low. In particular, when the remaining range is 50-100 km, the hazard rate for 50-100 km trips drops from 12% to 5%. We take this as evidence of range anxiety: even though the remaining range is sufficient to cover the planned distance, drivers forgo some trips for fear of depleting the battery before charging. Similarly, the hazard rate for trips between 50-100 km drops from 0.05 to 0.02 when the remaining range is 100-150 km.

Appendix Figure A3 plots hazard rates separately for morning trips, weekend trips, winter trips, and summer trips. Across all subsamples, the same pattern emerges: hazard rates are lower at low SOC, implying more forgone trips and consistent with range anxiety.

Figure 6: Charging behavior by remaining battery: with or without home chargers



Notes: This figure plots the distribution of charging events by the remaining percentage of battery at the start of an event. The solid blue line shows home charging for users with home chargers, while the dashed blue line indicates their fast charging behavior. The dashed red line represents users without home chargers. Charging at very low battery levels is disproportionately concentrated among those without home chargers, while users with home chargers tend to charge more frequently at higher remaining battery levels.

Lastly, drivers with home charging exhibit distinct patterns from those without. Those with home chargers primarily charge at home and use public fast chargers occasionally (e.g., for long-distance trips). They are also more likely to initiate charging at higher remaining battery levels than drivers without home chargers, likely reflecting the convenience of at-home charging.

3 Empirical Model

Our goal is to quantify range anxiety, which is difficult to measure directly based on observational data. We therefore develop a continuous-time dynamic model of EV driving and charging. This choice has two benefits. First, trips and charging events occur in continuous time. A continuous-time model allows us to directly exploit variations in event time intervals and avoids discretizing into coarse intervals (e.g. hours), thereby avoiding discretization bias. Second, when multiple charging and driving events fall within a short period, the continuous-time framework does not require imposing an order of events (which is often arbitrary), as the possibility that two events occur simultaneously at any instant is zero by construction. We present the model setup in Section 3.1, derive the Bellman equation in Section 3.2, and describe the estimation procedure in Section 3.3.

3.1 Setup

In the model, a representative driver of type i operates a car with a full range of $\bar{R}_i$. Trips arrive via a Poisson process. When a trip opportunity arrives, the driver decides whether to take the trip. Drivers earn utility from taking the trip. In the meantime, taking the trip shifts the state (for example, reducing the remaining battery or moving from a location with convenient charging to a location with less convenient charging). At the same time, charging opportunities also arrive via a Poisson process, and drivers decide whether to charge given the current state (such as the charging price level). Charging restores the battery capacity to its full level.[6] The key model elements are summarized below.

Consumer Types There are I different consumer types. Within each type i, consumers are homogeneous. Each consumer type i is determined by a triplet: the full battery range of the car ($\bar{R}$), the charging network size (N, either in 2021 or 2024), and whether the consumer has access to home chargers (H).

State Variable There are six state variables. The first state variable is the remaining battery range level: $b = \{1, ..., 10\}$, which represents the ten bins of the remaining battery range level: 0-50 km, 50-100 km, ..., 450-500 km. The second state variable is location convenience: $r = \{1, 2, 3, 4\}$, where we have grouped the log(charging access) measure ($CA_i = \sum_j \frac{1}{dist_{ij}^2}$) into four bins. The third state variable is the charging price: $p = \{1, 1.3, 1.5, 2\}$ (¥/kWh), corresponding to the four most commonly observed tiers of charging prices. The fourth state variable is only relevant to consumers with home chargers: $h = \{0, 1\}$, which takes the value of 1 if the location is near a home (or private) charger. The fifth state variable is the indicator of peak time $k = \{0, 1\}$, which is defined as the morning time (8 am- 8 pm). And the last state variable is the amenity access to the two POIs based on two categories "food" and "shopping". We group the log(charging access) measure ($CA_i = \sum_j \frac{1}{dist_{ij}^2}$) into four bins. Altogether, there are a total of $\mathbb{S} = \mathbb{B} \times \mathbb{R} \times \mathbb{P} \times \mathbb{H} \times \mathbb{K} \times \mathbb{A}$ ($10 \times 4 \times 4 \times 2 \times 2 \times 4 = 2,560$) different state values. The main specification of the paper focuses on the first four state variables, while as a robustness check, we include the peak time and amenity access.

Trip Arrival and Decisions A trip in our model is characterized as an event that changes the state from s to s'. The transition probability from state s to state s' is determined by trip

[6] In our sample, vehicle battery is restored to full capacity (defined as [90%, 100%] of the total battery capacity) 82% of the time. In a more general setting, one can assume that a charging event leads to a new battery level $r' > r$ with probability $p(r')$.

frequencies and the process that takes a driver from one state to another.

We use matrix Λ_r to denote the transition probabilities of the remaining battery range induced by trip events. Each entry $(b, b-j)$ in the matrix corresponds to the probability that the battery range moves from level b to level $b-j$ as a result of taking a trip with length j. As shown in Figure A3, the arrival rate of trips with varying length j (for $j = 0, 1, \ldots, 9$) appears to be roughly constant and independent of the current battery level. In other words, a trip of length 0-50 km arrives at the same rate regardless of whether the vehicle's remaining driving range is 200 km or 400 km. Let λ_j denote the arrival rate of a trip with length j. The transition matrix Λ_r exhibits a Toeplitz structure: it is a lower-triangular matrix with constant values along each sub-diagonal. Specifically, $\Lambda_r = \begin{bmatrix} \lambda_0 & 0 & 0 & \cdots & 0 \\ \lambda_1 & \lambda_0 & 0 & \cdots & 0 \\ \lambda_2 & \lambda_1 & \lambda_0 & \cdots & 0 \\ \vdots & \vdots & \vdots & \ddots & 0 \\ \lambda_9 & \lambda_8 & \lambda_7 & \cdots & \lambda_0 \end{bmatrix}$ All entries above the main diagonals are zero, since the battery level cannot increase without charging.

Matrix Λ_d denotes the transition probability of charging access. Each element $\lambda_{dd'}$ denotes the probability that a trip takes the driver from a location with charging access (d) to a new location with charging access (d'). Since there are four levels of charging access, Λ_d is a 4×4 matrix. Similarly, Λ_p denotes the transition probability of charging prices. Each element $\lambda_{pp'}$ denotes the probability that a trip moves from a location with charging price (p) to a new location with charging price (p'). Λ_p is also a 4×4 matrix. Finally, the probability of a trip arriving at home is given by Λ_h. As an extension, we can allow trip arrival rates to depend on peak time k: $\Lambda_r(k)$ to reflect more frequent trips in peak time. The joint trip arrival and peaktime transition follows the following structure: $\Lambda_{rk} = \begin{bmatrix} \lambda_{k=0\to k=0} & \lambda_{k=0\to k=1} \\ \lambda_{k=1\to k=0} & \lambda_{k=1\to k=1} \end{bmatrix} \bigotimes \begin{bmatrix} \Lambda_r(k=0) & 0 \\ 0 & \Lambda_r(k=1) \end{bmatrix}$.

Assuming the transition process of the four states is independent, the final transition matrix $q_{ss'}$ (state s to state s') is given by:

$$\mathbf{q} \equiv \Lambda_{rk} \bigotimes \Lambda_d \bigotimes \Lambda_p \bigotimes \Lambda_h \bigotimes \Lambda_a = \{q_{ss'}\}$$

The utility of taking a trip that moves from state s to state s' is given by:

$$\psi(1, s, s') = \alpha_0 + \alpha_1(b_r - b_{r'}) + \alpha_2 \mathbf{1}(r_{s'} = 2) + \alpha_3 \mathbf{1}(r_{s'} = 1) + \varepsilon_{d,1}.$$

where $r_{s'} = 2$ indicates that the remaining range after the trip is in the second bin, i.e., between [50km, 100km], and $r_{s'} = 1$ denotes the remaining range after the trip in the first

bin of [0km, 50km]. Utility for not taking the trip is normalized to zero: $\psi(0, s, s') = \varepsilon_{d,0}$. Parameter α_0 represents the baseline value of a trip, α_1 is the premium for long-distance trips, and α_2 and α_3 capture the anxiety of taking a trip leading to a very low remaining battery range.

We assume drivers always take the trip if the remaining battery level is above 300 km, corresponding to a cutoff $\chi = 6$. Essentially, we assume that range anxiety is irrelevant when the remaining battery is sufficiently high. If the remaining battery level is below 300 km, the driver decides on whether to take the trip based on the trip utility. If the utility shock ε_d has a type I extreme-value distribution, the policy of taking the trip is given by:

$$p_{\text{trip}} = \begin{cases} 1, & \text{if } x_r > \chi \\ \frac{\exp[(\psi(1,s,s')+V(s')]}{\exp[\psi(1,s,s')+V(s')]+\exp[\psi(0,s,s')+V(s)]}, & \text{if } x_r \leq \chi, \end{cases}$$

where $V(s)$ and $V(s')$ are value functions defined below. The realized (observed) trip frequency is given by: $\tilde{\mathbf{q}} = \mathbf{p} \times \mathbf{q}$.

Charging Arrival and Decisions The opportunity of charging arrives at rate λ_c. When a charging opportunity arrives, a driver decides whether to charge. If charging, he/she pays costs $c(1, s)$, and the remaining battery level increases to full capacity with probability 1. Other states are not affected b the charging event. Otherwise, the new state remains the same as the old state $s' = s$. We parameterize the charging costs as follows:

$$c(1, s) = \beta_0 + d_s\,\beta_1 + p_s\,\beta_2 + h_s\,\beta_3 + \varepsilon_{c,1}, \qquad c(0, s) = \varepsilon_{c,0},$$

where the coefficients β's are negative. With a slight abuse of notation, let $\bar{s} \equiv (r' = \bar{r},\, d,\, p,\, h)$ denote the state after charging when the battery is restored to full capacity.

Assuming the cost shock ε_c is distributed type-I extreme value, the probability to charge conditional on an opportunity arising is given by:

$$\pi_{\text{chg}}(s) = \frac{\exp\big(c(1, s) + V(\bar{s})\big)}{\exp\big(c(1, s) + V(\bar{s})\big) + \exp\big(V(s)\big)}.$$

Other Modeling Elements We assume that the flow utility $u(s) = 0$. That is, utility only comes from trips. We set the continuous-time discount rate at $\rho = 0.1/365 = \frac{1}{\delta} - 1$ per day, which corresponds to the discrete-time discount rate of $\delta = 0.999726$ per day, or 0.9 per year.

3.2 Bellman Equation

The Bellman equation characterizes the value function $V(s)$ in a continuous-time decision process where transitions occur stochastically. To gain intuition, consider a short time window Δt. The agent accrues an immediate utility flow $u(s)\Delta t$, which is assumed 0 in our setting. With probability $q_{ss'}\Delta t$, a trip opportunity that changes the state from s to s' arises. If the agent takes the trip, he/she gains the trip utility $\psi(s, s')$. The continuation value changes to the new state $V(s')$. Additionally, charging events occur with arrival rate λ_c, and the agent decides whether to charge the vehicle to maximize the future continuation value net of charging costs. The probability of nothing arriving and remaining in state s is $1 - \sum_{s' \neq s} q_{ss'}\Delta t - \lambda_c \Delta t$. We discount all future rewards at rate ρ. The resulting Bellman equation is:

$$
\begin{aligned}
V(s) = u(s) \times \Delta t + \sum_{s'} \frac{q_{ss'}\Delta t}{1+\rho\Delta t} E \max_{j\in\{0,1\}} \left\{ \underbrace{\psi(j=1,s,s') + V(s') + \varepsilon_{d,1}}_{\text{travel}}, \underbrace{\psi(j=0,s,s) + V(s) + \varepsilon_{d,0}}_{\text{not travel}} \right\} \\
+ \frac{\lambda_c \Delta t}{1+\rho\Delta t} E \max_{j\in\{0,1\}} \left\{ \underbrace{c(j=1,s) + V(\bar{s}) + \varepsilon_{c,1}}_{\text{charging}}, \underbrace{V(s) + \varepsilon_{c,0}}_{\text{not charging}} \right\} \\
+ \frac{1 - \sum_{s'} q_{ss'}\Delta t - \lambda_c \Delta t}{1+\rho\Delta t} V(s).
\end{aligned}
$$

This equation approximates a continuous-time Hamilton-Jacobi-Bellman (HJB) equation as $\Delta t \to 0$. Solving the equation for $V(s)$ yields:[7]

$$
\begin{aligned}
V(s) = & \frac{\sum_{s'} q_{ss'} \left\{ \log \left[\exp(\psi(1,s,s') + V(s')) + \exp(V(s')) \right] + \gamma \right\}}{\lambda_c + \rho + \sum_{s'} q_{ss'}} \\
& + \frac{\lambda_c \log \left[\exp(c(1,s) + V(\bar{s})) + \exp(V(s)) \right] + \lambda_c \gamma}{\lambda_c + \rho + \sum_{s'} q_{ss'}}
\end{aligned} \tag{1}
$$

3.3 Estimation Details

We follow a two-step estimation procedure. In the first step, we recover the state arrival and transition by estimating a hazard-rate model based on the observed trip arrivals and transitions and the time interval between these events. In the second step, we evaluate the

[7] Details about the derivation can be found in the Appendix.

empirical likelihood of observed trips and charging events at different states. The estimation procedure is similar to the discrete-choice dynamic model, but the main advantage is that we make use of the time interval between events in a continuous manner (via the hazard rates) and do not need to specify the order of each event.

Estimating Arrival Rates and Transition Probabilities Let q_{kl} denote the hazard rate of transitioning from state k to l, where a state is a quadruple that consists of battery level, charging access, charging price, and whether location is near home. As consumers may exhibit range anxiety and forgo trips that lead to low battery levels, the observed transition frequencies to low battery level may be lower than otherwise. To address this, we estimate the transition probabilities using trips with initial remaining range $>$ 300km, where it is probably reasonable that range anxiety is irrelevant.

The probability that the state changes within τ units of time is:

$$1 - \exp\left[-\tau\left(\sum_{l\neq k} q_{kl}\right)\right], \tag{2}$$

and the probability that the state does not change within τ units of time is:

$$\exp\left[-\tau\left(\sum_{l\neq k} q_{kl}\right)\right] \tag{3}$$

This is the cumulative distribution function (cdf) of the exponential distribution with a rate parameter equal to the sum of the exogenous state transition rates and the hazards of the player. Differentiating with respect to τ yields the density for the time of the next state change, which is the exponential probability density function with the same rate parameter:

$$\left(\sum_{l\neq k} q_{kl}\right)\exp\left[-\tau\left(\sum_{l\neq k} q_{kl}\right)\right]. \tag{4}$$

Define g to be the exponential term restated as a function of h: $g(\tau, k; \lambda) = \exp\left[-\tau\left(\sum_{l\neq k} q_{kl}\right)\right]$. The corresponding likelihood of nature moving the state from k to l is: $q_{kl}g(\tau, k; \lambda)$.

Now consider a continuous time sample of M agents making N state transitions in the sample. Define $I_{mn}(0, l)$ as the indicator for whether the n-th move of driver m to state l due to the trip arrival, and $I_{mn}(1, l)$ if the arrival to state l is due to charging or period n is the last observation in the sample period. Define $\tau_{mn} \equiv \underline{t}_{mn} - \bar{t}_{m,n-1}$ to be the holding time between

two events. For the interval between the last event and the end of the sampling period, we define the final state and interval length as $k_{m,T+1} \equiv k_{m,T}$ and $\tau_{m,T+1} \equiv \bar{T} - t_{mT}$. Then, the maximum likelihood estimates of the hazards $\mathbf{q}$ are:

$$\hat{\mathbf{q}} = \arg\max_{h \in \mathcal{H}} \left\{ \sum_{m=1}^{M} \sum_{n=1}^{T} \left[\sum_{l} (I_{mn}(0,l)) \left(\ln g\left(\tau_{mn}, k_{mn}; \mathbf{h}\right) + \ln q_{kl} \right) \right] + \sum_{l} (I_{mn}(1,l)) \ln g\left(\tau_{mn}, k_{mn}; \mathbf{h}\right) \right\}$$

The last term is the natural log of one minus the exponential cdf to account for the fact that another state change was not observed before a charging event.

Estimating Structural Parameters Given structural parameters $\theta = \{\boldsymbol{\alpha}, \boldsymbol{\beta}\}$ and hazard rates estimated in the first stage, we can solve the state-dependent value function via value function iteration as defined in (1): $T : V(k) \to V(k)$.

The probability of charging the vehicle and taking a trip is a function of estimated hazard rate $\hat{\mathbf{q}}$ and structural parameters $\theta = \{\boldsymbol{\alpha}, \boldsymbol{\beta}\}$. Specifically, the probability of charging is:

$$\hat{\pi}_{i1k}(\hat{\mathbf{q}}, \theta) = \frac{\exp[c(1,s) + \sum_k p_{sk} V(k)]}{\exp[c(1,s) + \sum_k p_{sk} V(k)] + \exp(c(0,s) + V(k))}$$

The joint likelihood of the next state change occurring after an interval of length τ and being the result of driver i taking charging action j is

$$\hat{\pi}_{ijk}(\hat{\mathbf{q}}, \theta) \hat{g}(\tau, k; \hat{\mathbf{q}}, \theta)$$

In addition, drivers decide on taking the trip or not. The probability that a driver takes a trip is:

$$\hat{p}_{i1ks}(\hat{\mathbf{q}}, \theta) = \frac{\exp[\psi(1,k,s) + V(s)]}{\exp[\psi(1,k,s) + V(s)] + \exp(V(k))} \text{ if } b_s \leq \chi$$
$$\hat{p}_{i1ks}(\hat{\mathbf{q}}, \theta) = 1 \text{ if } b_s > \chi$$

The joint likelihood of the next state change occurring after an interval of length τ and being the result of driver i taking traveling action $j = 1$ to state s is

$$\underbrace{\hat{q}_{ks} \hat{p}_{i1ks}(\tilde{\mathbf{q}}, \theta)}_{\tilde{q}_{iks}} \hat{g}(\tau, k; \tilde{\mathbf{q}}, \theta)$$

For driver m and all the observed actions n (trip/charging), we define $I_{mn}(c,j) = 1$ if the

state change at period n is a result of charging decision, $I_{mn}(t,j)=1$ if the state change at period n is a result of traveling decision to state s. The second stage MLE estimates can be written as:[8]

$$\hat{\theta}=\arg\max_{\theta}\left\{\sum_{m=1}^{M}\sum_{n=1}^{T}\left[\ln\hat{g}\left(\tau_{mn},k_{mn};\hat{\mathbf{q}},\theta\right)+\sum_{i}\sum_{j\neq 0}[I_{mn}(c,j)]\ln\hat{\pi}_{ijk}(\hat{\mathbf{q}},\theta)\right.\right.$$
$$\left.\left.+\sum_{i}\sum_{j\neq 0}[I_{mn}(t,j)]\ln\tilde{q}_{iks}(\hat{\mathbf{q}},\theta)\right]+\ln\hat{g}\left(\tau_{m,N+1},k_{m,N+1};\tilde{h},\theta\right)\right\}$$

4 Estimation Results

The goal is to recover hazard rate parameters: $\mathbf{q}=\{q_{jk}\}$ (state transition probabilities), and structural parameters $\{\boldsymbol{\alpha},\boldsymbol{\beta}\}$. The results are shown in Table 1, Table 2, and Figure 8.

4.1 Model Estimates

Trip Arrival Estimates. Since drivers with a home charger might have different traveling patterns from drivers without a home charger, we report the trip frequencies and state transition probabilities first for drivers without a home charger (67% of the drivers) and then separately for those with a home charger in Table 1. The trip patterns appear qualitatively similar, though drivers with a home charger are more likely to take trips that end in areas with less charging access.

The top panel of Table 1 reports the estimated Poisson arrival rates of trips per day, segmented by driving distance. The estimates reveal that short trips are much more frequent than long ones: trips under 50 km occur at a rate of 2.64 per day, while 50–100 km trips occur at 1.41 per day. In contrast, trips exceeding 200 km are rare, with arrival rates quickly dropping below 0.05 per day. This pattern aligns with observed EV usage behavior, where drivers most commonly make short-distance trips for commuting and errands, and only occasionally undertake long-range travel due to range limitations, planning requirements, and charging constraints. We additionally report the full specification with peaktime and amenity as state variables in the Appendix Table A3. The numerical patterns appear similar.

Trip Transition Frequencies. The bottom three panels of Table 1 document empirical frequencies of arriving at different types of destinations, defined by charging access measure

[8]For the interval between the last event and the end of the sampling period, we define the final state and interval length as $k_{m,T+1}\equiv k_{m,T}$ and $\tau_{m,T+1}\equiv\bar{T}-t_{mT}$.

Table 1: Model Estimates: State Arrival & Transition

	W/out H.C.		W/ H.C.	
	Estimate	SE	Estimate	SE
Trip Arrival (per day)				
<50km	2.8316	(0.0165)	2.7081	(0.0105)
50-100km	1.2479	(0.0108)	1.0021	(0.0066)
100-150km	0.2263	(0.0047)	0.1127	(0.0022)
150-200km	0.0941	(0.0030)	0.0323	(0.0012)
200-250km	0.0382	(0.0021)	0.0101	(0.0007)
250-300km	0.0193	(0.0020)	0.0037	(0.0006)
300-350km	0.0099	(0.0014)	0.0013	(0.0003)
350-400km	0.0043	(0.0013)	0.0007	(0.0004)
400-450km	0.0000	(4.1094)	0.0000	(2.3447)
Probability to a location (2021)				
Pr(->CA $\in [0,1]$)	0.4181	(0.0033)	0.5037	(0.0024)
Pr(->CA $\in [1,2]$)	0.3277	(0.0032)	0.3130	(0.0023)
Pr(->CA $\in [2,3]$)	0.1443	(0.0024)	0.1213	(0.0016)
Pr(->Price $\in [0,1.2]$)	0.2498	(0.0031)	0.2617	(0.0022)
Pr(->Price $\in [1.2,1.5]$)	0.1717	(0.0026)	0.2017	(0.0020)
Pr(->Price $\in [1.5,2]$)	0.2968	(0.0032)	0.2733	(0.0022)
Probability to a location (2024)				
Pr(->CA $\in [0,1]$)	0.1719	(0.0024)	0.2256	(0.0019)
Pr(->CA $\in [1,2]$)	0.0984	(0.0019)	0.1741	(0.0017)
Pr(->CA $\in [2,3]$)	0.2555	(0.0028)	0.2770	(0.0020)
Pr(->Price $\in [0,1.2]$)	0.2887	(0.0029)	0.2754	(0.0020)
Pr(->Price $\in [1.2,1.5]$)	0.1849	(0.0025)	0.2272	(0.0019)
Pr(->Price $\in [1.5,2]$)	0.2700	(0.0029)	0.2471	(0.0019)
Probability to home charger				
Pr(->W/ Private Charger)	0.8015	(0.0020)	0.8015	(0.0020)

Notes: The Number of observations is 8000 drivers with 214,000 sessions. The table reports estimated Poisson trip arrival rates and transition probabilities by types (with or without home chargers, under the 2021 or 2024 network).

(CA) and charging price, in 2021 and 2024. In 2021, a higher share of trips went to low-access, high-price areas— possibly reflecting uneven network development. By 2024, the trip usually led to locations with good charging access, indicating improved spatial distribution of the charging network.

Trip Utility Parameters. The top panel of Table 2 presents structural parameters governing the utility of taking a trip as a function of trip distance. The base utility of short trips ($\alpha_0 = 2.8549$) is high, reflecting the fact that trips are routine and often necessary and forgoing

Table 2: Model Estimates: Structural Primitives

	Main spec		Peak hour + Amenity	
Parameter	Estimate	SE	Estimate	SE
Trip utility				
α_0 (baseline trip utility)	2.4794	0.0129	3.4473	0.0264
α_1 (marginal utility per km)	0.8492	0.0155	0.7842	0.0202
α_2 (anxiety: 50–100 km remaining)	-0.7866	0.0206	-0.2254	0.0198
α_3 (anxiety: 0–50 km remaining)	-1.9079	0.0372	-1.9304	0.0373
α_4 (utility to high amenity)	—	—	0.0729	0.0073
Charging cost: consumers w/out home chargers				
β_0 (base cost)	-2.5790	0.0263	-4.0509	0.0267
β_1 (sensitivity to charging access)	0.6942	0.0100	0.7194	0.0100
β_2 (sensitivity to charging price)	-1.4823	0.0164	-1.4900	0.0167
β_3 (sensitivity to amenity)	—	—	0.1353	0.0057
Charging cost: consumers w/ home chargers				
when using fast charger:				
β_0^h (base cost)	-4.4177	0.0257	-4.7738	0.0274
β_1^h (sensitivity to charging access)	0.0641	0.0130	0.0510	0.0134
β_2^h (sensitivity to charging price)	-0.7196	0.0162	-0.8154	0.0172
when using home charger:				
β_3^h (base cost)	-0.2715	0.0184	-0.1650	0.0176
β_4^h (sensitivity to charging access)	-0.0087	0.0116	0.0408	0.0114
β_5^h (sensitivity to charging price)	-1.6274	0.0316	-1.5289	0.0307

Notes: The number of observations is 8,000 drivers with 214,000 sessions. Table 1 reports estimated Poisson trip arrival rates by types (with or without home chargers) across trip characteristics and destination cost intervals. Table 2 reports the estimated structural parameters: Consumers without home chargers: $C(\text{charging}, s) = \beta_0 + \beta_1(\text{CA}) + \beta_2(\text{price}) + \beta_3(\text{amenity})$. Consumers with home chargers: $C(\text{charging}, s) = \mathbb{1}(\text{not home}) \times (\beta_0^h + \beta_1^h(\text{CA}) + \beta_2^h(\text{price})) + \mathbb{1}(\text{home}) \times (\beta_3^h + \beta_4^h(\text{CA}) + \beta_5^h(\text{price}))$. Utility from trips: $\psi(\text{trips}, k, s) = \alpha_0 + \alpha_1(\text{trip distance}) + \alpha_2 \mathbf{1}(b_k \in [50, 100]) + \alpha_3 \mathbf{1}(b_k \in [0, 50]) + \alpha_4(\text{amenity})$, where b_k denotes remaining range after trip.

trips are costly. Longer trips are more valuable ($\alpha_1 = 0.7992 > 0$. Trips leading to low battery level generate disutility. In particular,($\alpha_2 = -0.7512$ for (50–100 km) , $\alpha_3 = -1.9424$ for 0–50 km). These estimates help rationalize the steep drop in observed realized trip frequencies for trips that lead to low battery levels.

Charging Cost Estimates The middle panel of Table 2 summarizes estimates for the cost of charging for drivers without home chargers. The baseline fixed cost of initiating a charge is negative ($\beta_0 = -2.55$), indicating that consumers incur a hassle cost around ¥51 per fast-charging (assuming 30 kWh per charge). However, this disutility is mitigated when

a charging station is conveniently located nearby: $\beta_1 = 0.70$ shows that increasing charging access significantly reduces the perceived cost. In contrast, high prices impose a substantial penalty, as indicated by $\beta_2 = -1.48$. These estimates are consistent with economic intuition in the data pattern: consumers value convenience and are sensitive to charging prices, especially when they are not urgently in need of energy. Based on the structural estimates, we can compute the elasticity of charging given a uniform increase in the charging price (in all stations) to be -0.98.

The bottom panel of Table 2 summarizes estimates for the cost of charging for drivers with home chargers. Home drivers can choose to charge with a slow charger (if they are at home) or a fast charger. The hassle cost of charging at home is close to zero ($\beta_3^h \approx 0$), while the hassle cost of charging at fast chargers is much more expensive ($\beta_0^h = -4.46$, or ¥184 per fast-charging assuming 30 kWh per charge). Consumers are less sensitive to fast charging prices ($\beta_2^h = -0.72$) perhaps because less familiarity with fast-charging networks) but more sensitive to home charging (electricity) prices ($\beta_5^h = -1.85$). Charging access is irrelevant for home charging and matters for fast charging, but much less so ($\beta_1^h = 0.06$). Overall, for consumers with home chargers, the average elasticity of charging probability with respect to charging price is -0.90, and therefore, they are less price sensitive.

The specification with amenity and peakhour as state variables deliver similar results in terms of price elasticity and hassle cost of charging. We find a slightly smaller range anxiety for trips that lead to 50-100km remaning range, which may be due to people feel less anxious if their EVs are in the lower range at off-peak time. We also find a positive but economically small effect of amenity access on charging utility, indicating that station convenience is likely the key factor that reduce the charging cost.

Model fit Model fit is validated in Figure 7 and our model captures the key features in the data: range anxiety reflects the missing trips that lead to low remaining ranges, quickly diminishing charging probability as remaining range is large, sensitivity to price, and local charging access.

4.2 Estimated Policy Functions

Figure 8 illustrates the estimated policy functions governing charging and travel decisions under various battery levels and station attributes. We have different types of consumers, and we start by reporting drivers with an EV full range of 500km, without home chargers (relying on fast chargers), and fixing the station network size at the 2024 level.

Panel (a) shows that the probability of charging declines as the remaining range increases, consistent with rational battery management behavior. However, this decline is highly sensitive to both station access and price: drivers are most likely to charge when stations are dense and prices are low (blue dashed line), and least likely when stations are sparse and prices are high (yellow dashed line). This confirms that both accessibility and affordability play important roles in charging behavior.

Panel (b) extends the analysis by comparing charging probabilities across consumers with different battery types. The curves are closely aligned, suggesting that the general shape of the charging policy is preserved across EVs with different maximum ranges. However, vehicles with greater battery capacity is less likely to charge given the same remaining battery ratio, indicating advantages of larger battery.[9] But they are more likely to charge given the same remaining range because the higher option value of recharging to the full range.

Panel (c) plots the same function as Panel (a), but shows consumers with home chargers deciding whether or not to take a fast-charging opportunity. Consumers are very unlikely to charge when the remaining range is high (> 200 km) because they have the home charging as the back-up option. Consumers are also less sensitive to prices or access, perhaps because they use these stations less frequently, and they would use them only in rare and urgent occasions.

Panel (d) shows consumers with home chargers decide whether or not to take a fast-charging opportunity. The decision rules are quite different— because home chargings are convenient so consumers tend to charge even when the remaining range is very high. Consumers are still sensitive to peak-load pricing and are more likely to charge at off-peak hours.

Appendix Figure A4 presents the estimated travel policy as heat maps. Cells report the conditional probability of taking a trip that transitions the remaining range from the x-axis value to the y-axis value, holding other location attributes fixed. Panel (a) considers trips from the most attractive origins (low prices, high access) to the least attractive destinations; probabilities are near zero at low remaining range, indicating pronounced range anxiety under poor charging conditions. Panel (b) reverses the direction—least attractive to most attractive—and probabilities are high even at very low remaining range, consistent with more observed trips toward cheaper, better-served areas at low remaining range. Overall, the policy is highly responsive to both remaining range and location variation in charging prices and access.

[9] This is to say, a car with full range at 500km is less likely to charge when the remaining range is 250km (50%) compared to a car with full range at 400km to charge at 200 km (50%).

5 Quantification and Policy Simulations

We evaluate counterfactual changes in battery technology and charging infrastructure by monetizing the model's value function—interpreted as the lifetime utility of vehicle ownership. The two policy levers are battery capacity and public charging-station network size. Consumers' willingness to pay (WTP) for them stems from three channels: (i) more realized trips that were previously infeasible or forgone, (ii) lower charging hassle costs, and (iii) improved charge timing that reallocates charging toward cheaper, better-access locations. We also construct a narrowly defined range-anxiety metric as the dollar value of forgone trips, as a function of the full range of a car and the network size. Lastly, we collect cost data from ancillary sources to analyze optimal policy design.

5.1 From Value Function to WTP

To compute WTP, we focus on the value function for a car with full range $\bar{R}$ given station density N and home-charging access H: $V(s; N, \bar{R}, H)$, and evaluate it at the steady state of the continuous-time Markov process.[10] We use a vector $\pi(s)$ denoting the probability of being at state s at any point of time:

$$V = \sum_s \pi(s) V(s)$$
$$\text{where } \pi \times Q = \pi,$$

where Q is a transition rate matrix, a function of $\tilde{\mathbf{q}}$ and charging rates $\mathbf{h}$.[11] We numerically simulate $\frac{dV}{dp}$ and this allows us to convert the value function changes to money as the changes in charging prices by computing $\Delta p = \Delta V / \frac{dV}{dp}$ at steady state.

If the model implied that a representative driver will give up Δp in charging price, the annual additional charging cost is: Lifetime WTP $= \Delta p \cdot \frac{D_{\text{year}}}{\bar{E}}$, where $\bar{E}$ is the average range per kWh of electricity and D_{year} is the longtime driving range of an EV. We further assume that $D = 20000 \times 8$, $\bar{E} = 6$. So we can convert the changes in charging prices to changes in lifetime WTP.

[10] For notation simplicity, we write $V(s)$ instead of $V(s; N, \bar{R}, H)$ but it should be taken as type-specific value function.

[11] In a continuous-time Markov process, the transition rate matrix Q describes the rate at which the process moves from one state to another, with each row summing to zero. The off-diagonal elements $q_{ij} \geq 0$ for $i \neq j$, and each diagonal element satisfies $q_{ii} = -\sum_{j \neq i} q_{ij}$, so that each row of Q sums to zero.

Decomposition Exercise We start with a decomposition exercise: how much does the WTP of driving an EV change from 2018 to 2021 to 2024? There are two major changes: (1) expansion of charging facility (from CA 2.08 to 2.84), (2) longer ranges (average ranges increase from 350km to 400km). Note that the average range increases do not apply to all EVs. Stock cars purchased in 2018 will not be affected by the improving battery technology, but they still benefit from the improved charging network. Due to the exponential growth of electric vehicle sales in Shanghai, only 13% of cars on the 2021 market were purchased prior to 2018, and 20% of cars on the 2024 market were purchased prior to 2021. In the main text, we focus on the aggregated welfare changes in Figure 9, while results disentangling stock and flow vehicles can be found in the Appendix Figure.

Main findings. Figure 10 shows monotonic increases in ΔWTP from 2018 to 2021 and 2024. The largest step occurs when public charging access rises (d: 18 → 21), while battery upgrades (b: 18 → 21 and b: 21 → 24) contribute smaller but positive increments. Gains are much larger for households without home chargers—about 2–4× those with home charging—reflecting their reliance on public infrastructure. Aggregating by observed home-charging shares, the weighted average reaches ≈ ¥30,000 by 2024 (¥62,000 for without home chargers and ¥18,000 for with home chargers).

5.2 WTP for Charging Access and Driving Range

To conduct counterfactual analysis, we fix the arrival probability of trips of different lengths and change the state variable to evaluate the new valuation function.

For battery sizes, we shift the full range $\bar{R}$ from 250km to 600km. This covers the range of most EVs on the market. The full battery capacity would affect the maximum range after a full recharge. For station access, we shift the probability of distribution of regions (from lowest access to highest access) in the following way: $\theta_r = [0.8, 0.2, 0.0, 0.0] + [-0.1, -0.02, 0.02, 0.1] \times r$ and $r \in \{1, 2, ..., 8\}$. So by shifting r up, we simulate a market with bad access to one with better access. For reference, the current average charging access at the 2021 level is 2.08, and the 2024 level is 2.84.

Panel (a) of Figure A9 reports lifetime WTP (in ¥) for joint increases in battery full range and network size (average charging access, CA). Values are normalized so that the baseline—250 km range and CA = 1.525—has ΔWTP = 0.

First, WTP rises quickly at low levels of range and CA and reaches economically meaningful sizes. For example, at 250 km and CA = 1.85, ΔWTP = 6,000 ¥, while at 600 km and CA

= 3.80 it reaches about 102,000 ¥.

Second, holding CA fixed at 1.525, raising the range from 250 to 300 km increases WTP by 22,000 ¥, whereas 550 to 600 km adds only 4,000 ¥. Holding range fixed at 250 km, increasing CA from 1.525→1.85 yields a gain of 6,000 ¥, while 3.475→3.80 adds 4,000 ¥. Thus, both range and network size display diminishing marginal value, though the extra benefits from range diminish faster.

Lastly, range and network size act as substitutes (negative cross-derivatives). From the baseline, increasing only the battery to 500 km yields 70,000 ¥; increasing only CA to 2.825 yields 22,000 ¥. Doing both together yields 85,000 ¥, which is less than the sum of separate effects (92,000 ¥). Intuitively, extra range is most valuable when access to charging is scarce, and improvements in charging access are most valuable when range is limited.

5.3 Quantifying Range Anxiety

In this section, we estimate the magnitude of range anxiety in monetary term, capturing the utility loss from forgone trips that are technically feasible but not taken due to fear of getting stranded on the road. In the model, α_2 and α_3 capture the disutility of taking trips that lead to a low battery. The utility losses from range anxiety are computed as the difference in the value function between the baseline model and a counterfactual where $\alpha_2 = 0$ and $\alpha_3 = 0$, and therefore all feasible trips are assumed to always be taken.

Figure 11 plots (monetized) range anxiety against the full driving range of the EV observed in the data for 2021 and 2024 separately. There is strong negative relationship between range anxiety and the driving range of an EV. For an EV with a driving range of 200km in 2021, the lower end of the range distribution, range anxiety amounts to ¥44,000 (or 44% of the EV price), but range anxiety reduces to only ¥3000 for an EV with a driving range of 450km. The comparison between 2021 and 2024 shows range anxiety shifts down for an EV of the same range from 2021 to 2024 due to improvement in charging access.On average, range anxiety amounts to ¥13,600 ($1,900), or 10% of the EV price in 2021. In 2024, range anxiety drops to ¥8,400 ($1,200), or 4% of the EV price. The reduction was driven by both the increase in EV driving range (from 353km to 388km), and the charging station network size (from 400 to 2,268 stations), with the former contributing to 80% of the drop in range anxiety.

To further illustrate the role of charging access in affecting range anxiety, the two dotted lines depict the level of range anxiety assuming the EV of a certain driving range only has the worst charging access (top) or the best charging access (bottom) observed in the data. Consistent with the intuition, charging access plays a bigger role for EVs with a low driving

range. For EVs with a range of 200km, improving charging access from the worst to the best can reduce range anxiety from ¥46,000 to ¥30,000, a 35% reduction.

Figure A5 presents range anxiety with respect to driving range separately for two groups of EVs: those without access to home charging in panel (a), and those with access in panel (b). Panel (a) shows that range anxiety shifts down from 2021 to 2024 for an EV with the same driving range, due to the improvement in charging access. However, there is no visible shift in range anxiety from 2021 to 2024 for those with home chargers as shown in Panel (b), suggesting more limited role of access to public charging in addressing range anxiety for those with access to home charging. Comparing the two panels, average range anxiety does not differ significantly between these two groups of EVs due to a combination of two countervailing forces: (1) access to home charging relieves range anxiety; and (2) those with access to home charging tend to be less sensitive to charging price as the parameter estimates suggest.

5.4 Optimal Policy Design and Complementarity

In this section, we first discuss how the social value and cost of charging facilities and battery range are computed. Then we will conduct counterfactual analyses to (1) compute the optimal bundle of the two facilities in different years, and show that the current average range in 2024 is below optimal, while the number of stations has exceeded the optimal number; (2) demonstrate the complementarity of investing in both charming facility and battery range at the same time because of the diminishing return of each, highlighting the value of industry-public collaboration in promoting electric vehicles.

Back-of-Envelope Calculations on Value of Battery Capacity We evaluate the economic benefit of increasing driving range by adding battery capacity and compare it with the associated cost. To translate battery capacity (kWh) into driving range (km), we adopt a constant conversion factor of $\bar{E} = 6$ km/kWh.[12]

In addition, we assume a lifetime driving distance D (in km). Then the amount of electricity consumed per year is: $E = \frac{D}{\bar{E}}$. As a sanity check, a reasonable model should yield comparable orders of magnitude between the lifetime benefit of bigger battery and cost from a bigger battery. The cost is estimated to be roughly \$155 per kWh around 2021 and \$115

[12]Other avenues to extend range— e.g., improvements in vehicle efficiency, aerodynamics, or thermal management— are outside the scope of this analysis; we hold them fixed and interpret the results as the value of additional battery capacity.

in 2024. Therefore, a 50 km increase in range would imply additional cost of $\frac{50 * \$115}{\bar{E}} =$ to $\frac{50 * \$155}{\bar{E}} =$ ¥6708 to 9042, which aligns well with the number of lifetime savings implied by the model in Figure A9.

Back-of-Envelope Calculations on Value of Network size We examine the economic benefit of adding an additional station to the Shanghai network. Each network will increase the average level of charging access with a diminishing return to scale. See Appendix Figure A6 for the detailed relationship. At the station level d, the additional value of one station is given by $\frac{\partial CA}{\partial d}$. And we can evaluate the WTP for the station given by $\frac{\partial CA}{\partial d}\frac{\partial V(range,CA)}{\partial CA}$.

The social cost of a station is computed based on the industry report.[13] Each charger costs from ¥231,000 in 2018 to ¥150,500 in 2024. We further assume 20 chargers per station, and 1 million potential EV drivers as the population to bear the cost. These two numbers guide us in designing the optimal number of charging stations for different types of consumers.

Trade-off Between Network size and Battery Range. To begin with, we solve the following optimization problem to get the optimal level of battery and network size at given social costs:

$$\max_{R,N} WTP(R,N) - \text{Battery Cost}(R) - \text{Charger Cost}(N) \tag{5}$$

Table 3 and Figure 12 report the optimal level, social welfare, and consumer WTP at the given level of a representative EV under the network in each given year.

Complementarity in investing in battery and charging network Although battery capacity and charging-network size are strategic substitutes in the model— an arbitrarily large battery would eliminate the need for public charging, and an extremely dense network would offset limited range, fast diminishing returns to each technology imply that investing in both in a coordinated way is more effective than investing in just one. Figure A7 illustrates the intuition, and Table 4 empirically evaluates the optimal expansion path compared with the expansion path with focus on only one technology, and the observed expansion path, and shows which sector Shanghai is lagging in different years.

[13]The sources can be found at https://pdf.dfcfw.com/pdf/H3_AP202212051580809140_1.pdf.

Table 3: Optimal Battery/Station Choices under Different Costs

Cost level	$\bar{R}_{\text{opt}}$ (km)	N_{opt}	Welfare	WTP	Cost
Panel A: w/ home c.					
2018	295	100	12.3	43.2	30.9
2021	368	100	29.3	60.4	31.1
2024	426	100	41.0	69.2	28.2
Panel B: w/out home c.					
2018	328	806	35.8	86.6	50.8
2021	417	1080	62.5	110.7	48.2
2024	484	1335	80.8	122.3	41.6
Panel C: weighted avg.					
2018	321	414	26.6	69.8	43.1
2021	404	825	50.7	94.3	43.6
2024	469	1158	67.3	106.1	38.8

Notes: Each panel corresponds to a consumer type. "Cost level" denotes the battery and station cost calculated for the year. We use grid search to find the optimal bundle $\{\bar{R} \in [250, 550], N \in [100, 2500]\}$. Welfare, WTP, and Cost are reported in thousands ¥, and are computed by comparing them with a car that has a full range of 200km and no fast-charging stations available.

6 Conclusion

Although range anxiety consistently emerges as a key barrier to EV adoption in consumer surveys, industry reports, and policy discussions, there has been little economic analysis quantifying its magnitude and evaluating the effectiveness of potential remedies. To our knowledge, this study is the first to micro-found range anxiety, the utility loss from unrealized but feasible trips due to fear of depleting power before reaching a charging station, within a continuous-time dynamic model of EV driving and charging behavior. Using high-frequency usage and charging data from 8,000 EVs in Shanghai, we estimate average range anxiety at $1,900 in 2021, declining to $1,200 in 2024. This decline is primarily driven by the expansion of the charging network (from 400 to 2,268 stations) and, especially, by improvements in EV driving range (from 353 km to 388 km) over this period.

Our simulations highlight the crucial roles of two approaches in addressing range anxiety: expanding driving range (through increased battery capacity) and enhancing charging access (through larger charging networks). Because each approach exhibits diminishing returns, the welfare-maximizing policy requires coordinated investment in both charging infrastructure and battery capacity. The socially optimal levels of charging network size and driving range evolve as the costs of charging-station construction and battery production decline over time. Our analysis indicates that the realized investment trajectory diverges significantly from the

Table 4: Complementarity of Battery ($\bar{R}$) and Network Size (N)

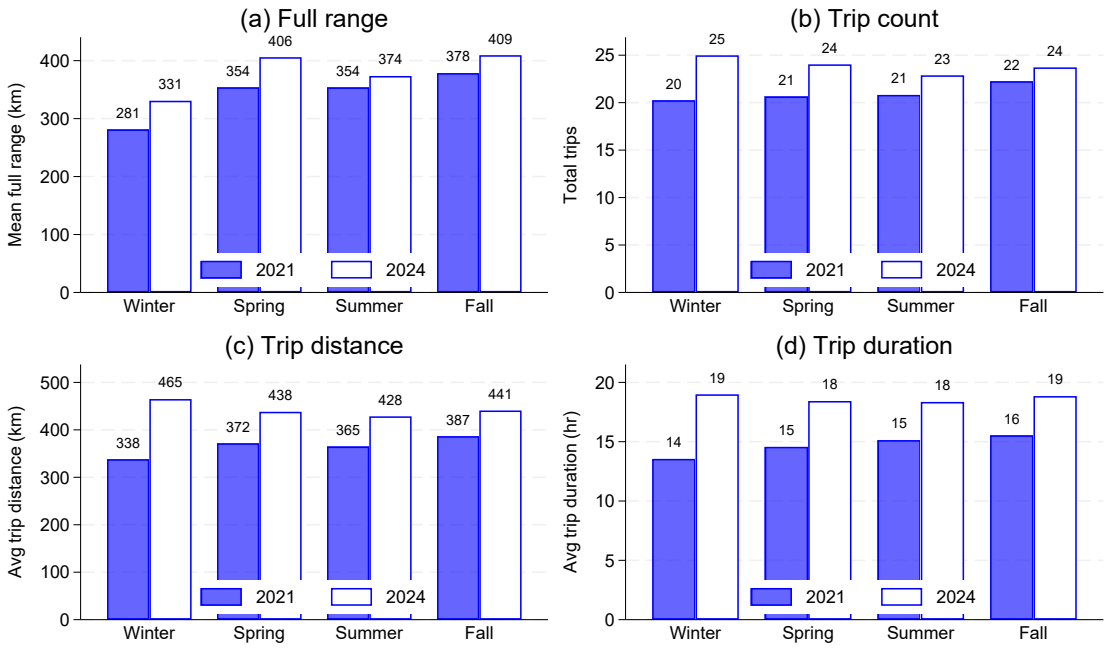
Scenario	$\bar{R}$ (km)	N	Welfare	WTP	Cost
Panel A: 2018 level of battery and station cost					
A: $(\bar{R}^{opt}, N^{opt})$	321	414	26.6	69.8	43.1
B: $(\bar{R}^{obs}, N^{obs})$	318	100	22.4	60.4	38.0
C: $(\bar{R}^{opt}, N^{obs})$	327	100	22.5	63.3	40.7
D: $(\bar{R}^{obs}, N^{opt})$	318	414	26.6	68.9	42.2
Panel B: 2021 level of battery and station cost					
A: $(\bar{R}^{opt}, N^{opt})$	404	825	50.7	94.3	43.6
B: $(\bar{R}^{obs}, N^{obs})$	353	400	47.7	78.6	30.9
C: $(\bar{R}^{opt}, N^{obs})$	411	400	49.7	91.2	41.5
D: $(\bar{R}^{obs}, N^{opt})$	353	884	49.1	84.0	34.9
Panel C: 2024 level of battery and station cost					
A: $(\bar{R}^{opt}, N^{opt})$	469	1158	67.3	106.1	38.8
B: $(\bar{R}^{obs}, N^{obs})$	388	2268	62.7	97.3	34.6
C: $(\bar{R}^{opt}, N^{obs})$	461	2268	64.9	108.4	43.5
D: $(\bar{R}^{obs}, N^{opt})$	388	1315	64.7	94.4	29.7

Notes: Each panel corresponds to cost levels in the indicated year. $(\bar{R}^{opt}, N^{opt})$ denotes the welfare-maximizing pair, $(\bar{R}^{obs}, N^{obs})$ fixes both at observed levels in each year, and mixed cases optimize only one dimension while holding the other fixed at observed. The welfare number is computed by comparing it with a car that has a full range of 200km and no fast-charging stations available.

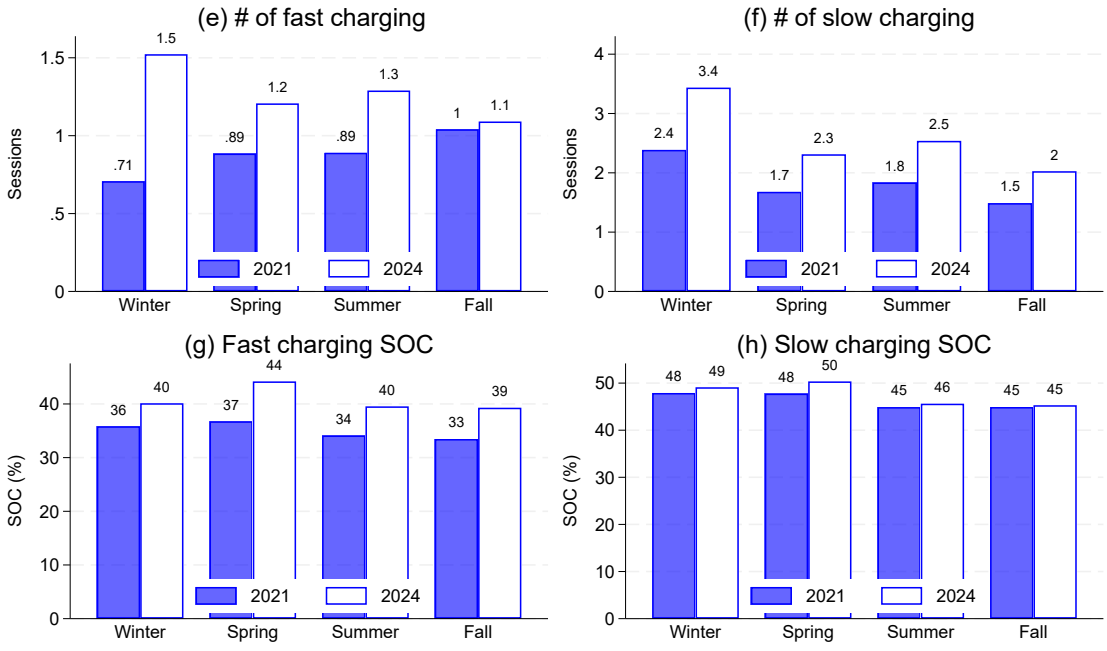
optimal path: by 2024, Shanghai has over-invested in charging infrastructure while under-investing in driving range relative to the social optimum.

We note two important caveats and directions for future research. First, our data and analysis are restricted to travel within Shanghai, and thus our estimates of range anxiety likely represent a lower bound, as range anxiety may be more pronounced for long-distance trips. That said, long-distance driving is less common in China than in countries such as the U.S., partly due to China's extensive high-speed rail system. Second, our empirical analysis is based on data from Shanghai, and the quantitative findings should be interpreted in that context. As detailed EV usage and charging data become available elsewhere, our framework can be adapted to quantify range anxiety and its policy implications across different settings, where underlying preferences may vary. Another important direction for future research is to leverage granular data to examine the optimal spatial distribution of charging infrastructure.

Figure 2: Data Description of EV usage dataset: 2021 vs. 2024



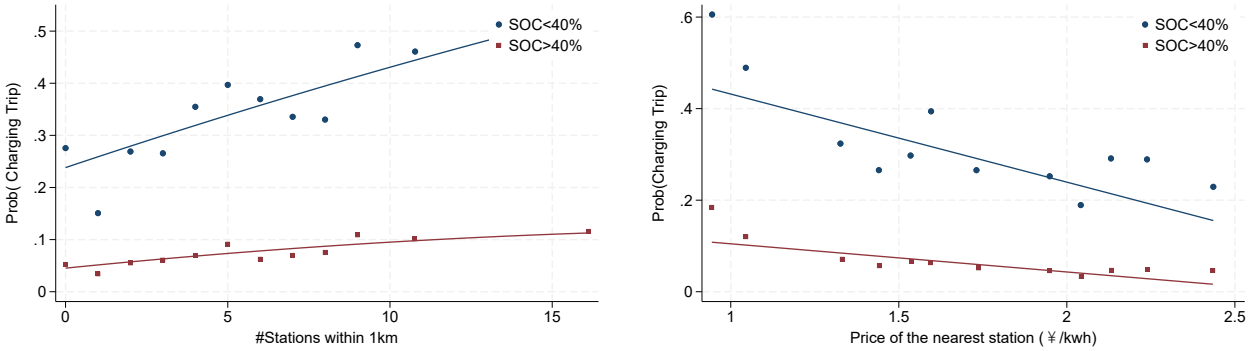
(a) Trip-related events



(b) Charging-related events

Note: The dataset in each year includes four weekly cross-sections of 1100 randomly selected representative EVs in Shanghai during a week in Jan (Winter), March (Spring), Aug (Summer), and Oct (Fall), respectively, for the years 2021 and 2024. The top panel reports vehicle range, weekly trip count, weekly distance, and weekly trip duration. The bottom panel reports the weekly fast charging and slow charging events, as well as SOC for fast charging and slow charging, respectively.

Figure 4: Charging Behavior as a Function of Charging Network and Price

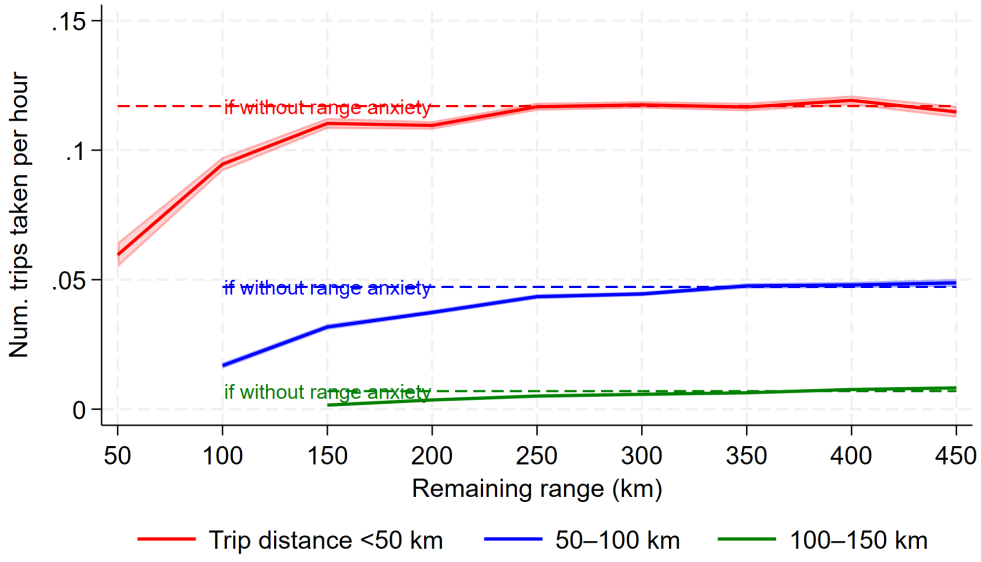


(a) Charging probability vs. local charging access

(b) Charging probability vs. price at nearest station

Note: these graphs examine how charging probability varies with local station access and price. Consumers are more likely to charge in areas with a dense network (Panel (a)) and low prices (Panel (b)). In both cases, the effect is stronger when the remaining battery (SOC) is below 40%.

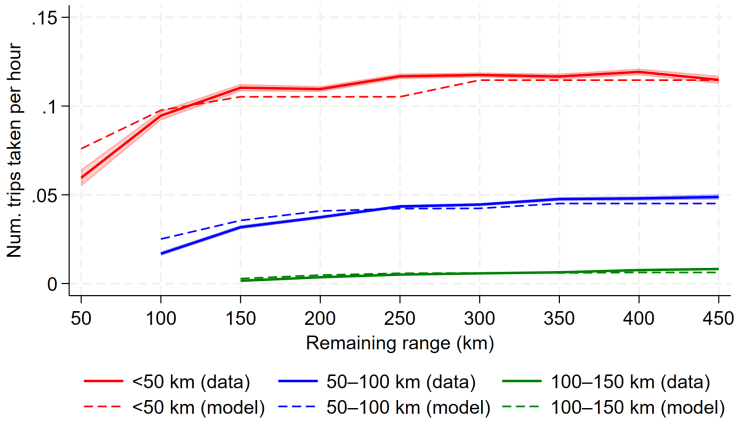
Figure 5: Range Anxiety: hazard rates of trip initiation by remaining driving range



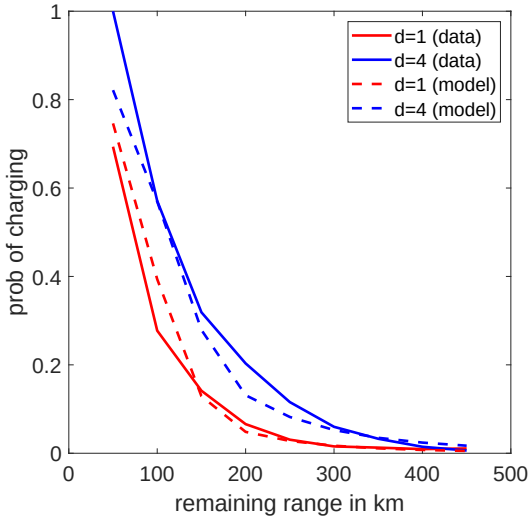
Note: Each colored line corresponds to a trip with a certain distance: $<$ 50 km, 50–100 km, 100–150 km, and 150–200 km. Hazard rates are computed as the number of trips initiated per hour from each starting remaining range (x-axis), normalized by the hours vehicles stay in that state (until a trip arrives). Shaded areas show 95% confidence intervals.

Figure 7: Estimated Trip-taking hazard rate (Model Fit)

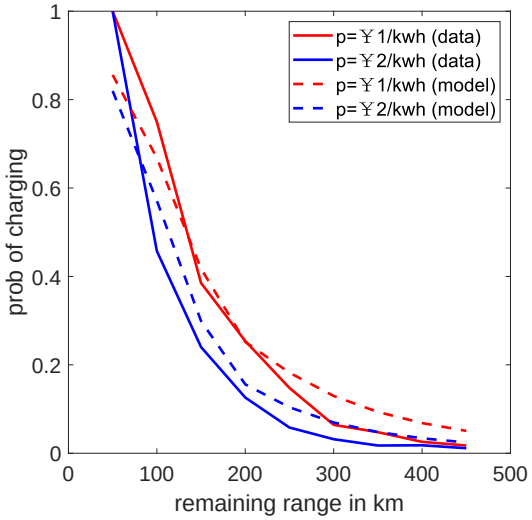
(a) Travelling policy by trip distance



(b) Charging policy by charging access



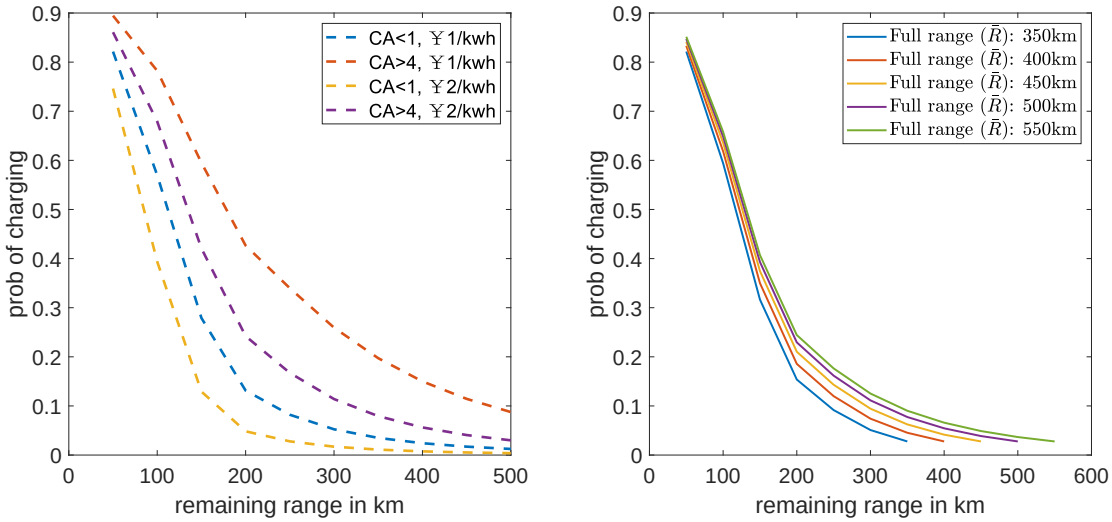
(c) Charging policy by charging price



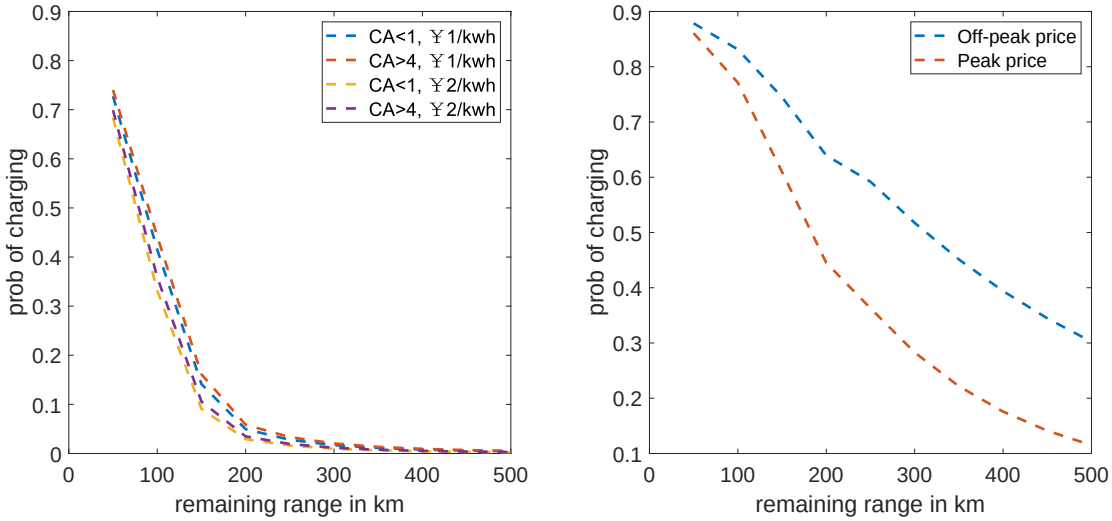
Notes: This figure presents the estimated policy functions governing charging and traveling decisions. Solid lines denote policy recovered from data, and dashed line denotes model estimates.

Figure 8: Estimated policy function $h(b, d, p, h)$

(a)$\pi^{H=0,\bar{R}=500}(r; d, p)$ (b) $\pi^{H=0,\bar{R}}(r)$

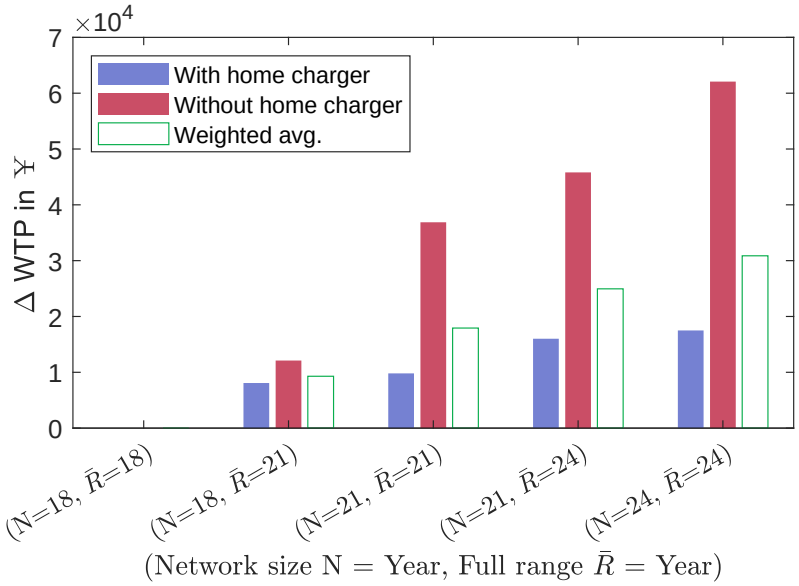


(c) $h^{H=1,\bar{R}=500}(r; d, p, h = 0)$ (d) $h^{H=1,\bar{R}=500}(r; d, p, h = 1)$



Notes: This figure presents the estimated policy functions $h(b, r, p, h)$ governing charging decisions as a function of b (remaining battery range), d (charging access), p (charging price), and h (home charger nearby). Panel (a) shows the charging probability for consumers without home chargers as a function of remaining range under four scenarios defined by price and station access. Panel (b) shows charging probabilities for consumers without home chargers across the different battery capacities. Panels (c) and (d) display the probability of charging for consumers with home chargers. The probability of using fast-charging is low (close to zero when range $>$ 200km). Charging at home is frequent even when the remaining battery is relatively high and during off-peak hours.

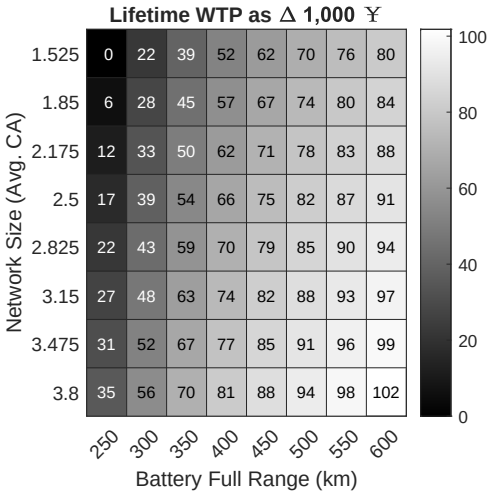
Figure 9: Decomposition of welfare gain: 2018 vs. 2021 vs. 2024



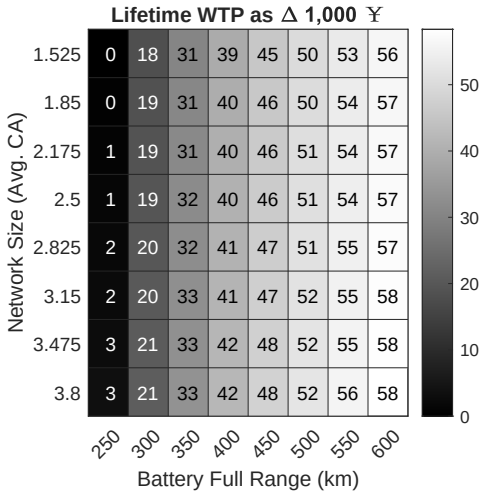
Note: Bars show ΔWTP (lifetime WTP, 10,000 ¥) relative to 2018 (N=18, $\bar{R}$=18) as $(N, \bar{R})$ are sequentially updated to 2021 and 2024: at each x-tick, first raise $\bar{R}$ holding N fixed, then raise N holding $\bar{R}$ fixed. Colors: blue = with home charger; red = without; green = sample-weighted mean (weights = observed home-charger shares at 67%).

Figure 10: WTP for driving range and charging access

(a) Δ WTP without home chargers

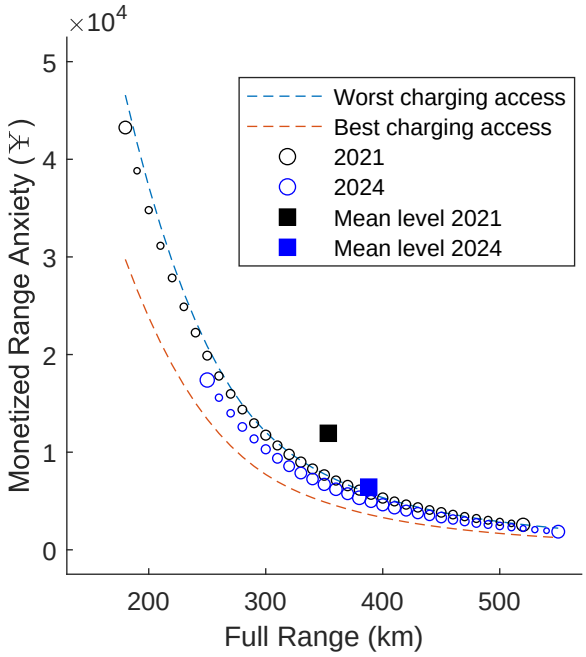


(b) Δ WTP with home chargers



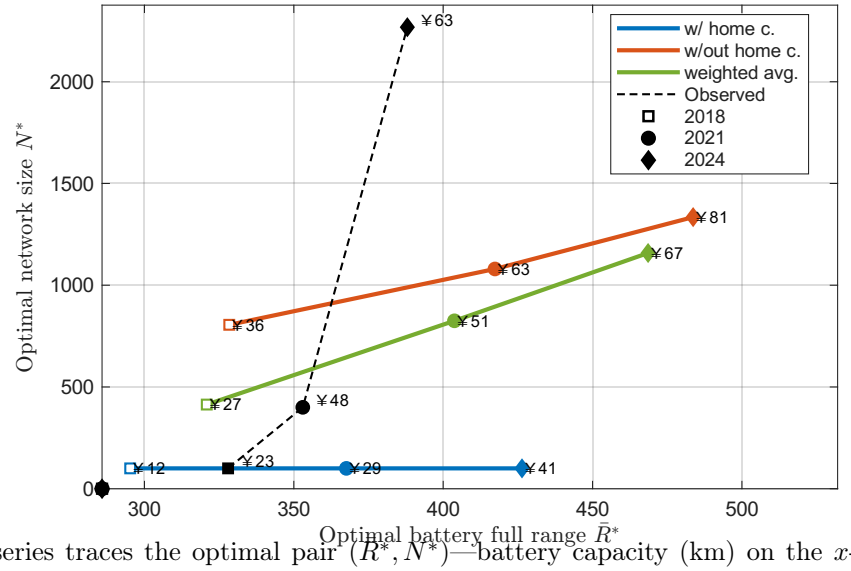
Notes: Figure (a) shows the estimated willingness to pay (WTP) for network size (or higher average charging access) and the full driving range, both expressed in terms of lifetime charging costs. The baseline in Panel (a) is 100% battery as the current level and the current charging access (CA) level. 2021 network has CA=2.08 and 2024 network has CA=2.84. Panel (b) shows the surplus loss from ("narrowly defined") range anxiety, i.e., people forgo trips that are technically feasible, computed as the difference of the value function when trips are always taken, converted to lifetime WTP.

Figure 11: Range Anxiety by Driving Range



Notes: Each panel plots *monetized range anxiety* (lifetime WTP, 10^4 ¥) against the vehicle's full range (km). Circle area is proportional to the empirical frequency of each full-range level in that year's EV sample. Filled squares mark the weighted mean level for the year. The downward slope indicates that range anxiety declines with battery range; the downward shift from 2021 to 2024 reflects improvements in network size (from 400 to 2268 stations) and full driving range (from 353 to 388km).

Figure 12: Optimal levels of Battery Range and Charging Network Size



Notes: Each series traces the optimal pair $(\bar{R}^*, N^*)$—battery capacity (km) on the x-axis and charging-network size index on the y-axis—for three cost environments (2018, 2021, 2024). Blue: consumers *with* home chargers; orange: *without* home chargers; green: sample-weighted average (weights are the observed home-charger shares). The dashed black line connects the *observed* $(\bar{R}, N)$ in the data. Markers indicate years: □ 2018, • 2021, ⋄ 2024. Currency labels next to the points report the model net surplus at the corresponding optimum (WTP minus cost, in 1,000 ¥). Connecting lines illustrate how optimal technology and infrastructure choices shift as battery and station costs change over time.

References

Arkolakis, Costas, Kenneth T. Gillingham, and Seung-Yong Yoo, "Optimizing Electric Vehicle Infrastructure," *AEA Papers and Proceedings*, May 2025, *115*, 563–67.

Bailey, Megan R., David P. Brown, Blake C. Shaffer, and Frank A. Wolak, "Show Me the Money! A Field Experiment on Electric Vehicle Charge Timing," *American Economic Journal: Economic Policy*, 2025, *17* (2), 259–284.

Barwick, Panle Jia, Christopher Knittel, Shanjun Li, Youming Liu, James Stock, and Binglin Wang, "Optimal Charging Infrastructure for Electric Vehicles," Working Paper 2025.

_ **, Hyuk-Soo Kwon, and Shanjun Li**, "Attribute-based Subsidies and Market Power: an Application to Electric Vehicles," Working Paper 32264, National Bureau of Economic Research March 2024.

Bernard, Louise, Andy Hackett, Robert Metcalfe, Luca Panzone, and Andrew Schein, "The Impact of Dynamic Prices on Electric Vehicle Public Charging Demand: Evidence from a Nationwide Natural Field Experiment," Technical Report, Centre for Net Zero May 2025. Working Paper.

Bloomberg Intelligence, "Global Battery Electric Vehicle Outlook," 2024.

Burlig, Fiona, James Bushnell, David Rapson, and Catherine Wolfram, "Low Energy: Estimating Electric Vehicle Electricity Use," *AEA Papers and Proceedings*, May 2021, *111*, 430–35.

Cabral, Luis, Chiara Gardenghi, Deepak Hegde, and Junrui Lin, "Public and Private Innovation: Complements or Substitutes?," *Columbia University Working Paper*, 2025.

Chokshi, Niraj, Matthew Goldstein, and Erin Woo, "Biden's electric car plans hinge on having enough chargers," *The New York Times*, 2021. Accessed: 2025-07-12.

Dorsey, Jackson, Ashley Langer, and Shaun McRae, "Fueling alternatives: Gas station choice and the implications for electric charging," *American Economic Journal: Economic Policy*, 2025, *17* (1), 362–400.

Garg, Teevrat, Ryan Hanna, Jeffrey Myers, Sebastian Tebbe, and David G. Victor, "Electric Vehicle Charging at the Workplace: Experimental Evidence on Incentives and Environmental Nudges," CESifo Working Paper 11445, CESifo, Munich 2024.

Heid, Pascal, Kevin Remmy, and Mathias Reynaert, "Equilibrium Effects in Complementary Markets: Electric Vehicle Adoption and Electricity Pricing," *TSE Working Paper*, 2024.

Jacqz, Irene and Sarah Johnston, "Electric Vehicle Subsidies and Urban Air Pollution Disparities," *Journal of the Association of Environmental and Resource Economists*, 2024, *11* (S1).

Klier, Thomas H. and James M. Rubenstein, "North America's Rapidly Growing Electric Vehicle Market: Implications for the Geography of Automotive Production," *Economic Perspectives*, December 2022, *No. 5.* Accessed: 2025-07-12.

La Nauze, Andrea, Lana Friesen, Kai Li Lim, Flavio M. Menezes, Lionel Page, Thara Philip, and Jake Whitehead, "Can Electric Vehicles Aid the Renewable Transition? Evidence from a Field Experiment Incentivising Midday Charging," CESifo Working Paper 11386, CESifo, Munich 2024.

Li, Jing, "Compatibility and investment in the us electric vehicle market," *Unpublished manuscript, MIT*, 2023.

_ **and Katalin Springel**, "Entry and Coordination in the U.S. Electric Vehicle Charging Industry," *Tufts Working Paper*, 2025.

Li, Shanjun, Lang Tong, Jianwei Xing, and Yiyi Zhou, "The market for electric vehicles: indi-

rect network effects and policy design," *Journal of the Association of Environmental and Resource Economists*, 2017, *4* (1), 89–133.

Liu, Zikun, "Policy Design for Sustainable Innovation and Adoption: A Structural Analysis of the Electric Vehicle Market," 2025. Working Paper.

Qin, Molin and Jonathan Scott, "The High Cost of Low Range: Estimating the Hidden Cost of Range Anxiety in Electric Vehicles," *Working Paper*, 2023.

Rainieri, Giuseppe, Chiara Buizza, and Alberto Ghilardi, "The psychological, human factors and socio-technical contribution: A systematic review towards range anxiety of battery electric vehicles' drivers," *Transportation Research Part F: Traffic Psychology and Behaviour*, 2023, *99*, 52–70.

Rapson, David S. and Erich Muehlegger, "The economics of electric vehicles," *Review of Environmental Economics and Policy*, 2023, *17* (2), 274–294.

Remmy, Kevin, "Adjustable Product Attributes, Indirect Network Effects, and Subsidy Design: The Case of Electric Vehicles," 2025. Working Paper.

Springel, Katalin, "It's Not Easy Being "Green": Lessons from Norway's Experience with Incentives for Electric Vehicle Infrastructure," *Review of Environmental Economics and Policy*, 2021, *15* (2).

_ , "Network externality and subsidy structure in two-sided markets: Evidence from electric vehicle incentives," *American Economic Journal: Economic Policy*, 2021, *13* (4), 393–432.

Wang, Yucheng, "Who Receives Environmental Benefits from Driving Electric Vehicles?," *Unpublished Manuscript*, April 2024.

Wardlaw, Christian, "What is Range Anxiety with Electric Vehicles?," J.D. Power November 2020. Accessed 2025-07-12.

Zhou, Yiyi and Shanjun Li, "Technology Adoption and Critical Mass: The Case of the U.S. Electric Vehicle Market," *The Journal of Industrial Economics*, 2018, *66* (2), 423–480.

Online Appendix

Appendix A. Derivation of Bellman Equation (1)

We begin by discretizing time into intervals of length Δt. Within each interval, four events may occur:

1. Flow utility: The agent receives instantaneous flow utility $u(s)\,\Delta t$ from remaining in state s during the interval.

2. Travel transition: With probability $q_{ss'}\Delta t$, the state transitions to $s' \neq s$ due to a travel event. Upon such a transition, the agent chooses between traveling ($j = 1$) and not traveling ($j = 0$), which yields the choice-specific values

$$\psi(1, s, s') + V(s') + \varepsilon_{d,1} \quad \text{or} \quad V(s) + \varepsilon_{d,0}.$$

3. Charging opportunity: With probability $\lambda_c \Delta t$, a charging opportunity arises. The agent then chooses whether to charge ($j = 1$) or not ($j = 0$), yielding the values

$$-c(1, s) + V(\bar{s}) + \varepsilon_{c,1} \quad \text{or} \quad V(s) + \varepsilon_{c,0}.$$

4. No event: With the remaining probability $1 - \sum_{s'} q_{ss'}\Delta t - \lambda_c \Delta t$, no travel or charging event occurs, and the state remains s.

Because the model includes discounting at a rate ρ, each continuation value is divided by $(1 + \rho\Delta t)$. Putting these components together gives:

$$\begin{aligned} V(s) = u(s)\,\Delta t &+ \sum_{s'} \frac{q_{ss'}\Delta t}{1 + \rho\Delta t} E \max_{j\in\{0,1\}} \Big\{\psi(1, s, s') + V(s') + \varepsilon_{d,1},\ V(s) + \varepsilon_{d,0}\Big\} \\ &+ \frac{\lambda_c \Delta t}{1 + \rho\Delta t} E \max_{j\in\{0,1\}} \Big\{ - c(1, s) + V(\bar{s}) + \varepsilon_{c,1},\ V(s) + \varepsilon_{c,0}\Big\} \\ &+ \frac{1 - \sum_{s'} q_{ss'}\Delta t - \lambda_c \Delta t}{1 + \rho\Delta t} V(s). \end{aligned}$$

This recursion is a discrete-time approximation to the continuous-time Hamilton–Jacobi–Bellman (HJB) equation, which becomes exact as $\Delta t \to 0$ following the two steps below:

Step 1. Simplifying the expectation terms With i.i.d. Type I extreme value shocks, the

expectation of the maximum is:

$$E \max_{j\in\{0,1\}} \{v_j + \varepsilon_j\} = \sigma \ln \left(\sum_j e^{v_j/\sigma} \right) + \gamma\sigma,$$

where γ is the Euler–Mascheroni constant. Normalizing $\sigma = 1$ gives:

$$E \max\{\psi(1, s, s') + V(s'),\, V(s)\} = \ln\Big(e^{\psi(1,s,s')+V(s')} + e^{V(s)}\Big) + \gamma,$$
$$E \max\{-c(1, s) + V(\bar{s}),\, V(s)\} = \ln\big(e^{-c(1,s)+V(\bar{s})} + e^{V(s)}\big) + \gamma.$$

Substituting the log-sum expressions into the recursion, we obtain

$$\begin{aligned} V(s) = u(s)\,\Delta t &+ \sum_{s'} \frac{q_{ss'}\Delta t}{1+\rho\Delta t} \Big\{ \ln\big(e^{\psi(1,s,s')+V(s')} + e^{V(s)}\big) + \gamma \Big\} \\ &+ \frac{\lambda_c \Delta t}{1+\rho\Delta t} \big\{ \ln\big(e^{-c(1,s)+V(\bar{s})} + e^{V(s)}\big) + \gamma \big\} \\ &+ \frac{1}{1+\rho\Delta t} \Big[1 - \sum_{s'} q_{ss'}\Delta t - \lambda_c \Delta t \Big] V(s). \end{aligned}$$

Notice that the last term comes from the probability of staying in the same state when neither a travel nor a charging event occurs. At this stage, every coefficient is scaled by Δt and discounted by $1 + \rho\Delta t$.

Step 2. Taking the $\Delta t \to 0$ limit. To simplify, multiply both sides by $(1 + \rho\Delta t)$:

$$\begin{aligned} (1+\rho\Delta t)V(s) = u(s)\,\Delta t &+ \sum_{s'} q_{ss'}\Delta t \Big\{ \ln\big(e^{\psi(1,s,s')+V(s')} + e^{V(s)}\big) + \gamma \Big\} \\ &+ \lambda_c \Delta t \Big\{ \ln\big(e^{-c(1,s)+V(\bar{s})} + e^{V(s)}\big) + \gamma \Big\} \\ &+ \Big[1 - \sum_{s'} q_{ss'}\Delta t - \lambda_c \Delta t \Big] V(s). \end{aligned}$$

Bring the last term on the right-hand side together with the left-hand side:

$$\begin{aligned} (1+\rho\Delta t)V(s) - \Big[1 - \sum_{s'} q_{ss'}\Delta t - \lambda_c \Delta t \Big] V(s) = u(s)\,\Delta t \\ + \sum_{s'} q_{ss'}\Delta t \Big\{ \ln\big(e^{\psi(1,s,s')+V(s')} + e^{V(s)}\big) + \gamma \Big\} \\ + \lambda_c \Delta t \Big\{ \ln\big(e^{-c(1,s)+V(\bar{s})} + e^{V(s)}\big) + \gamma \Big\}. \end{aligned}$$

Simplify the coefficient on $V(s)$:

$$\big[(1+\rho\Delta t) - (1 - \sum_{s'} q_{ss'}\Delta t - \lambda_c \Delta t)\big] V(s) = (\rho + \lambda_c + \sum_{s'} q_{ss'})\Delta t\, V(s).$$

Dividing both sides by Δt and taking the limit as $\Delta t \to 0$, we obtain:

$$\begin{aligned}(\rho + \lambda_c + \sum_{s'} q_{ss'})V(s) = u(s) + \sum_{s'} q_{ss'}\Big\{ \ln\big(e^{\psi(1,s,s')+V(s')} + e^{V(s)}\big) + \gamma\Big\} \\ + \lambda_c\Big\{ \ln\big(e^{-c(1,s)+V(\bar{s})} + e^{V(s)}\big) + \gamma\Big\}.\end{aligned}$$

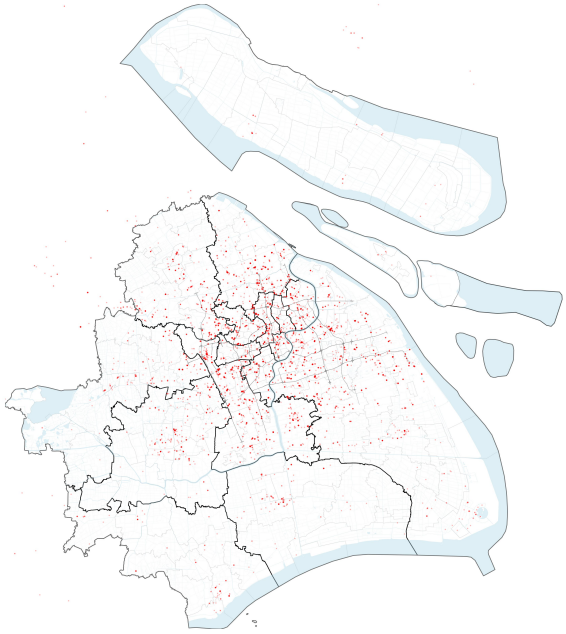
Dividing both sides gives (note we assume $u(s) = 0$):

$$\begin{aligned}V(s) = \frac{\sum_{s'} q_{ss'}\Big\{ \ln\big(e^{\psi(1,s,s')+V(s')} + e^{V(s)}\big) + \gamma\Big\}}{\rho + \lambda_c + \sum_{s'} q_{ss'}} \\ + \frac{\lambda_c\Big\{ \ln\big(e^{-c(1,s)+V(\bar{s})} + e^{V(s)}\big) + \gamma\Big\}}{\rho + \lambda_c + \sum_{s'} q_{ss'}},\end{aligned}$$

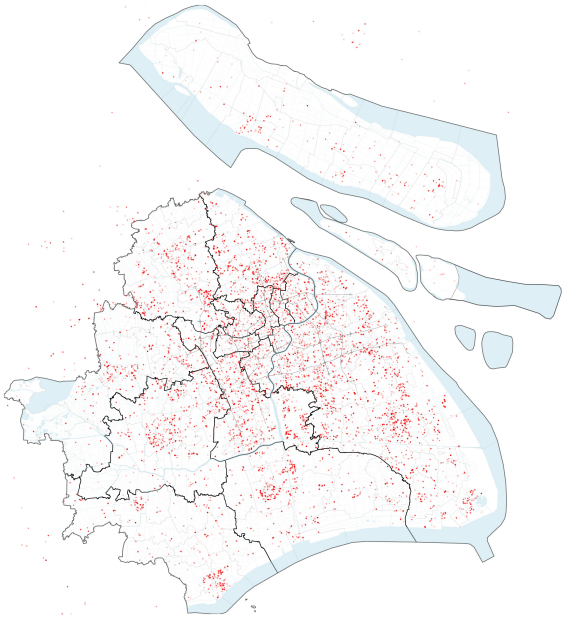
which matches Equation (1).

A Appendix Figures

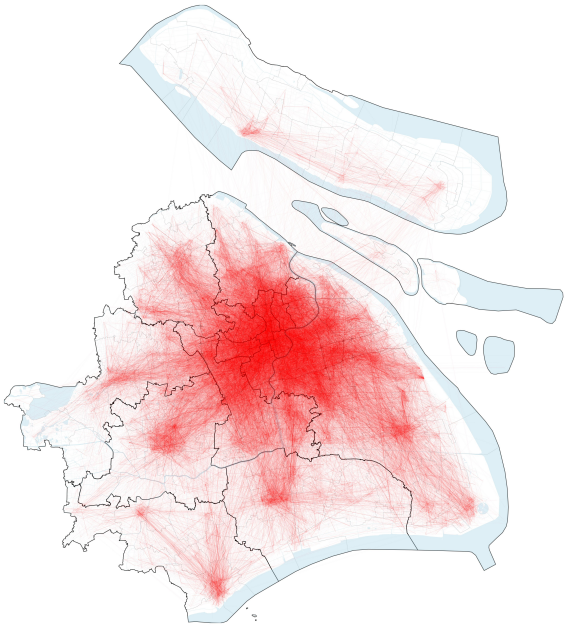
Figure A1: Descriptions of the EV Trip dataset



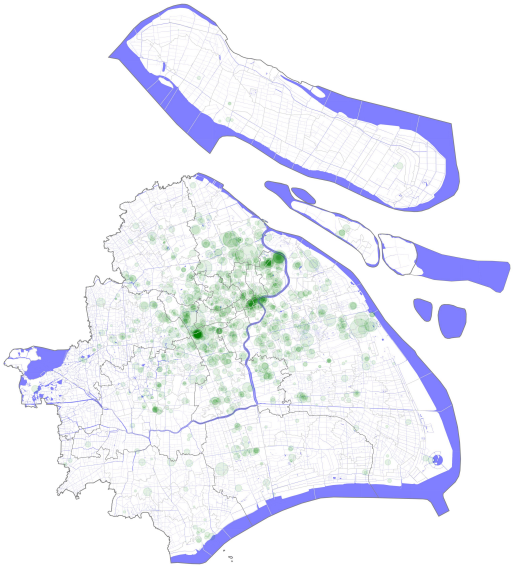
(a) Fast Charging Locations



(b) Slow Charging Locations



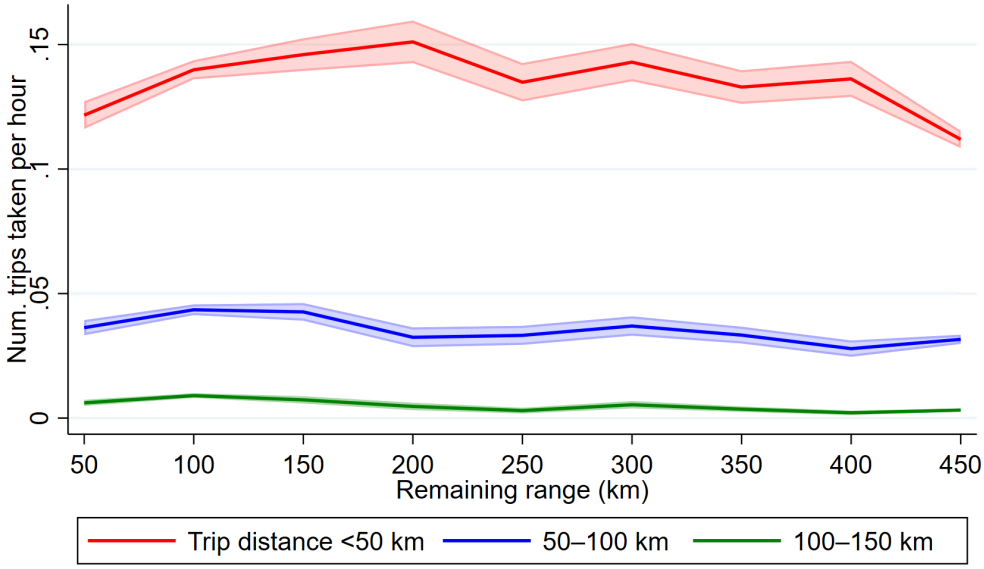
(c) Trip: Origin to Destination



(d) Fast Stations (weighted by usage)

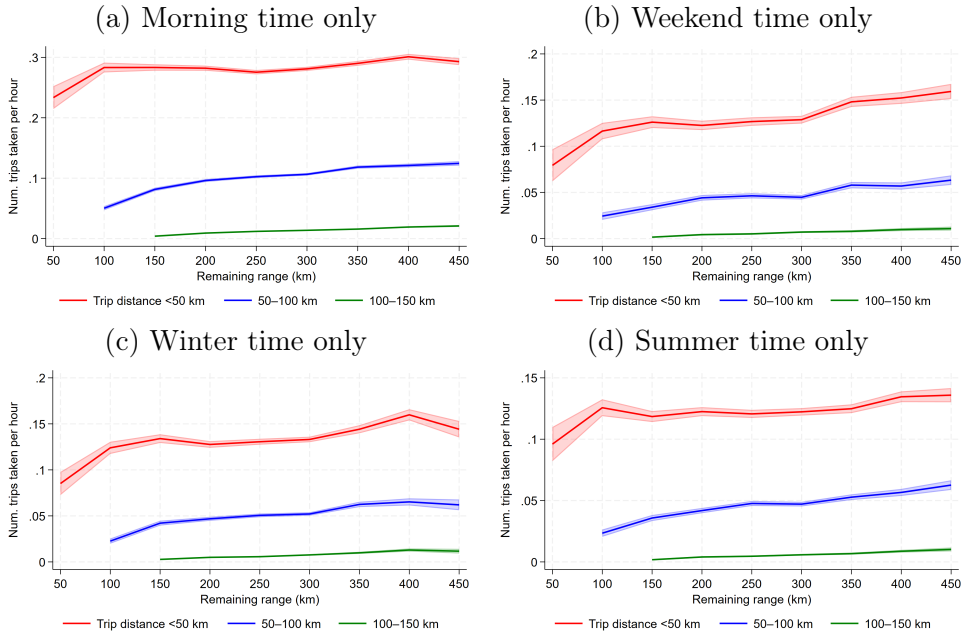
Note: Figures (a)-(c) are constructed based on the eight-week EV charging sample. Figure (a) plots locations of the observed 8,524 fast charging; Figure (b) plots the locations of the 16,986 observed slow charging; Figure (c) plots the connected lines of 188,707 trip origins to destinations (excluding trips outside Shanghai for visualization). Figure (d) plots the fast charging station usages in 2024 from the charging network dataset sourced from Shanghai Electric Technology Center, and it aligns well with Figure (a), verifying the representativeness of the trip sample.

Figure A2: Placebo: No Missing Trips at Low SOC for PHEVs



Notes: Each colored line corresponds to a trip with a certain distance: < 50 km, 50–100 km, 100–150 km, and 150–200 km. Hazard rates by the y-axis are computed as the number of trips initiated per hour from each starting remaining range (x-axis), normalized by the hours vehicles stay in that state (until a trip arrives). Shaded areas show 95% confidence intervals. Each panel presents the results for a specific time frame. The overall pattern is consistent with that from pooling all the data together.

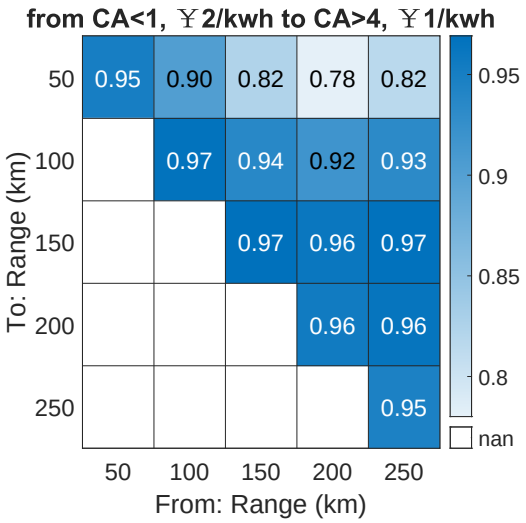
Figure A3: Unrealized Trips at Low SOC



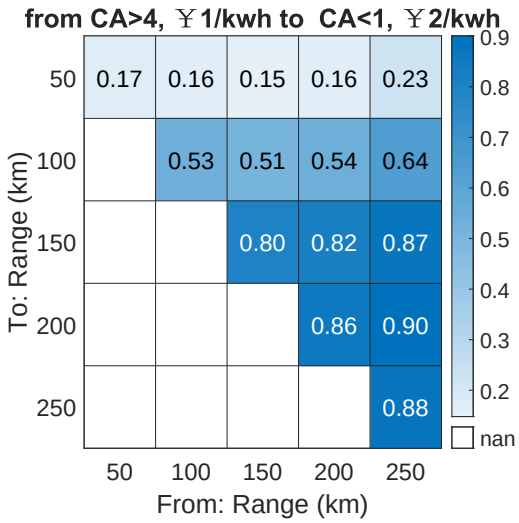
Notes: Each colored line corresponds to a trip with a certain distance: < 50 km, 50–100 km, 100–150 km, and 150–200 km. Hazard rates by the y-axis are computed as the number of trips initiated per hour from each starting remaining range (x-axis), normalized by the hours vehicles stay in that state (until a trip arrives). Shaded areas show 95% confidence intervals. Each panel presents the results for a specific time frame. The overall pattern is consistent with that from pooling all the data together.

Figure A4: Estimated Trip-taking policy function $h^{H=0,\bar{R}=500}(b, r, p)$

(a) Travelling policy



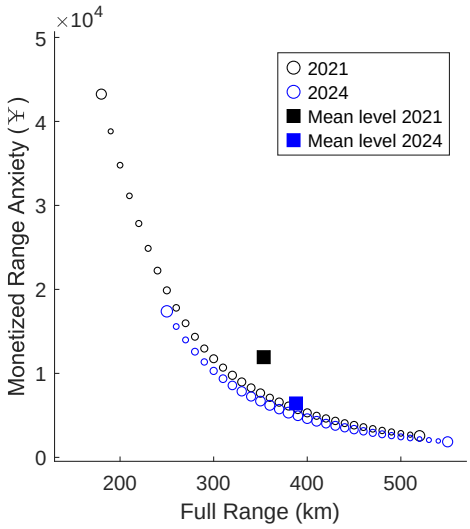
(b) Travelling policy



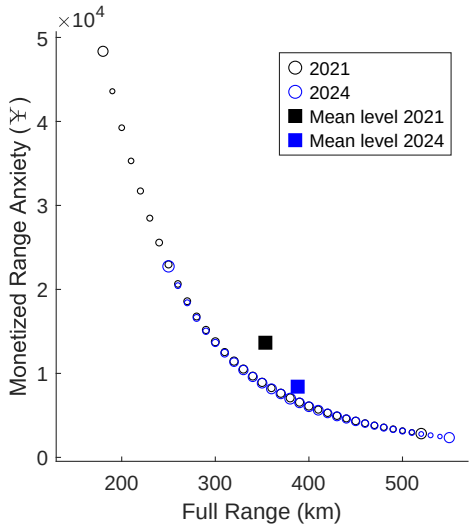
Notes: This figure presents the estimated policy functions governing charging and traveling decisions. Panels (a) and (b) display the probability of taking a trip with a starting range (x-axis) to an end range (y-axis). "Nan" denotes infeasible trips. Darker shades represent higher probabilities. Each heatmap cell corresponds to the probability of taking the trip that moves the car from a given initial range (x-axis) to a new remaining range (y-axis).

Figure A5: Range Anxiety by Access to Home Charging

(a) Range anxiety w/o home chargers

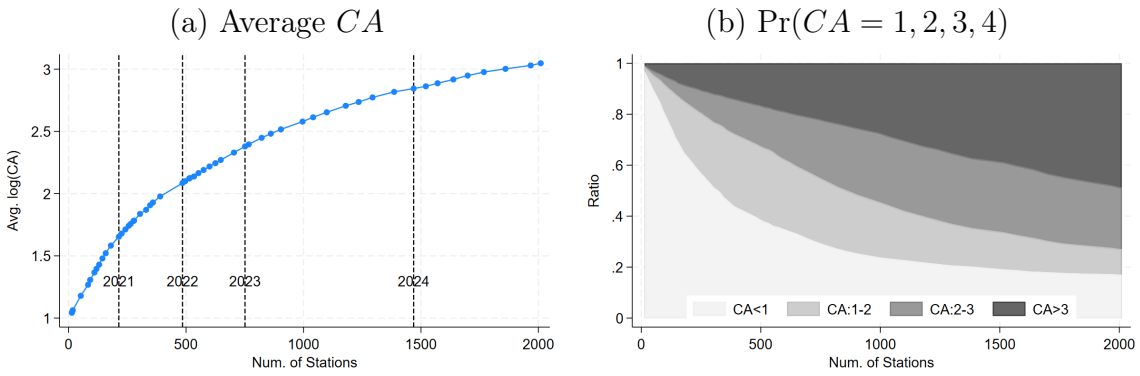


(b) Range anxiety with home chargers



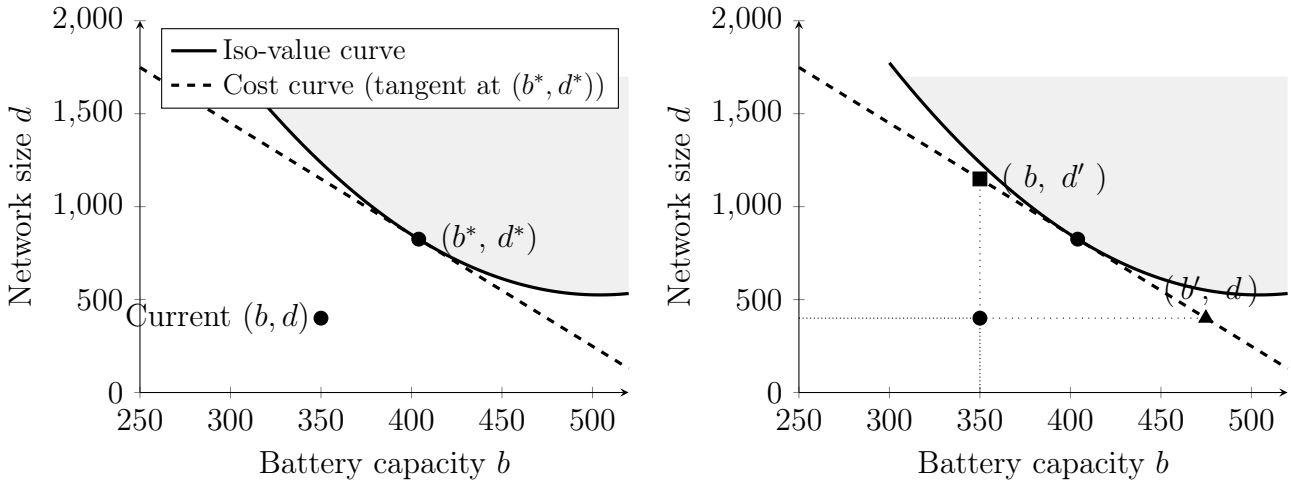
Notes: Each panel plots *monetized range anxiety* (lifetime WTP, 10^4 ¥) against the vehicle's full range (km). Circle area is proportional to the empirical frequency of each full-range level in that year's sample. Filled squares mark the weighted mean level for the year. Panel (a) evaluates consumers *without* home charging; panel (b) evaluates consumers *with* home charging. The downward slope indicates that range anxiety declines with battery range; the downward shift from 2021 to 2024 reflects improvements in network size and prices.

Figure A6: Relationship between charging access and number of stations



Notes: Charging access (CA) is an inverse–distance–squared index for each location i, $\text{CA}_i = \sum_j 1/\text{dist}_{ij}^2$, where nearby stations receive more weight. **Panel (a)** plots the sample average of log(CA) as the total number of stations increases; the vertical dashed lines mark the observed station counts in 2021–2024. The concavity indicates diminishing marginal improvements in access as the network grows. **Panel (b)** shows how the cross-sectional distribution of access shifts with network size: stacked areas are the shares of locations falling in four CA bins (< 1, 1–2, 2–3, > 3).

Figure A7: Policy coordination between battery capacity and network density.



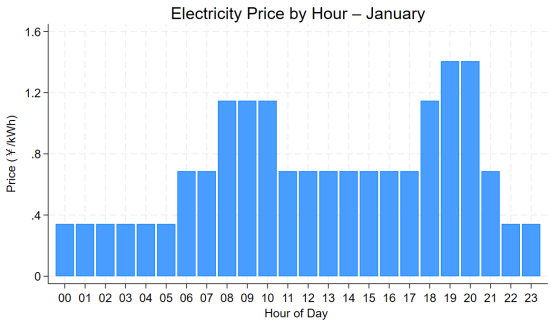
(a) Iso-value (solid) and cost (dashed); optimum at tangency.

(b) One-dimensional moves along the cost line: improve only d (to d') or only b (to b').

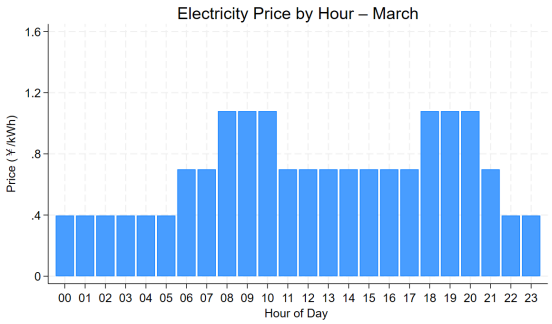
Notes: The figure illustrates **policy coordination** between battery capacity b and charging-network size d. The solid curve is an iso-value (welfare) contour: combinations above the curve (light shading) deliver higher welfare. The dashed line is the *cost* trade-off—here drawn as the tangent at the optimum (b^*, d^*)—representing budgets or relative prices that keep total cost constant along the line. **Panel (a)** shows the optimum at the tangency of the iso-value and cost curves; the current configuration (b, d) lies below that level set. **Panel (b)** decomposes incremental policies from the current point: moving vertically to (b, d') improves only network size, while moving horizontally to (b', d) improves only battery capacity, both along the same cost line. Because b and d exhibit diminishing marginal returns, coordinated investments that move (b, d) toward the tangency typically achieve larger welfare gains than one-sided changes that adjust only b or only d.

Figure A8: Commercial Electricity Price by months

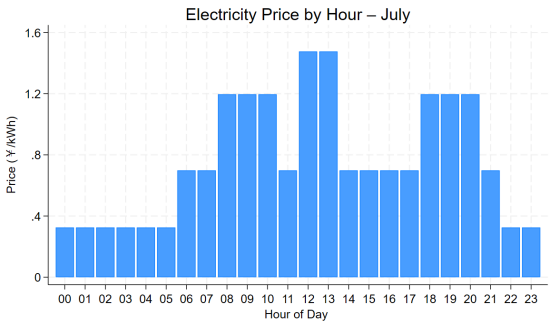
(a) January



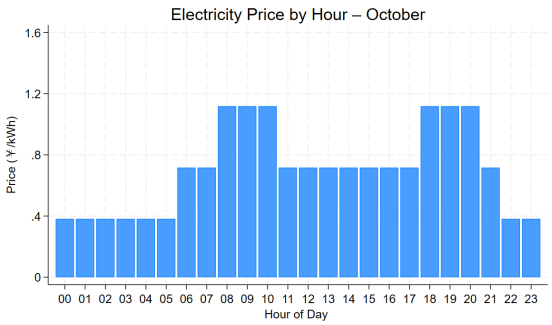
(b) March



(c) July



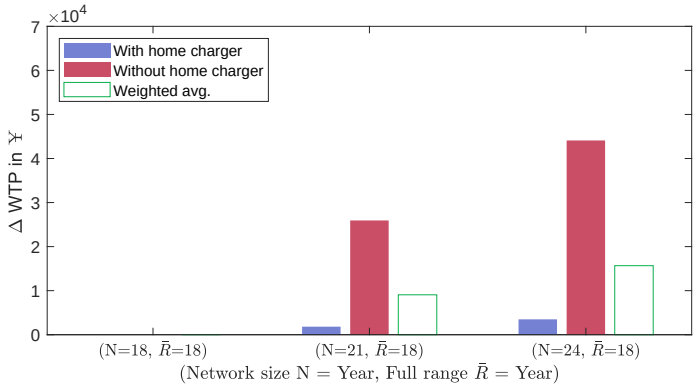
(d) October



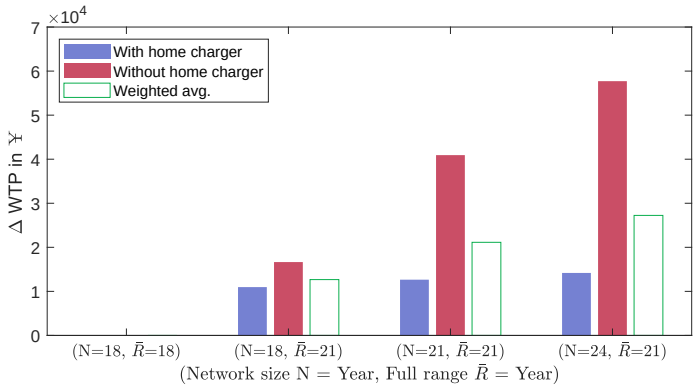
Notes:

Figure A9: Decomposition for EV purchased in different years

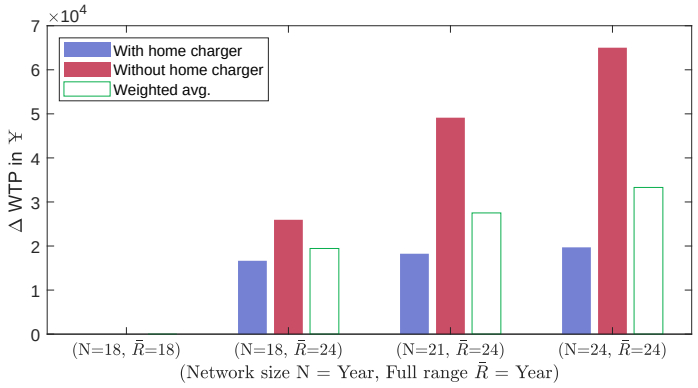
(a) An average EV bought in 2018



(b) An average EV bought in 2021



(c) An average EV bought in 2024



Notes: Figures (a) to (c) plot the surplus gains of an EV with different ranges and networks. The baseline is an average car purchased in 2018 with a 2018 charging network.

B Appendix Tables

Table A1: Dataset Overview

Year	2021				2024			
	Winter	Spring	Summer	Fall	Winter	Spring	Summer	Fall
Driver info								
# Drivers	1100	1100	1100	1100	1100	1100	1100	1100
Avg. range (km)	293	357	356	381	332	411	378	416
With home charger	75.1%	61.9%	62.8%	57.2%	67.0%	64.8%	66.7%	63.5%
Driving Trips per driver per week								
Count	20.9	20.3	20.5	20.9	23.4	21.6	21.7	21.7
Total distance (km)	376.4	388.5	381.8	405.6	477.2	447.1	447.6	514
Total duration (hour)	15.6	16.3	15.8	16.1	19.2	18.4	18.8	19
Chargings per driver per week								
# Fast	0.7	0.9	0.9	1.1	1.5	1.2	1.3	1.1
# Slow	2.5	1.9	1.9	1.6	3.5	2.4	2.6	2.1
Fast Duration (hour)	2.3	1.6	1.7	1.9	2.1	1.8	1.8	1.7
Slow Duration (hour)	14.7	13	13.3	11.7	13.6	11	12.4	12.2
Fast Starting SOC	35	37	34	33	40	44	39	39
Slow Starting SOC	47	48	45	45	49	50	46	45

Note: The dataset in each year includes four weekly cross-sections of 1100 randomly selected EVs from the EV stock in Shanghai during Jan 23-30 (Winter), March 20-27 (Spring), Aug 23-30 (Summer), and Oct 20-27 (Fall). In total, there are 188,707 driving trips, about 16,986 slow charging sessions, and about 8,524 fast charging sessions. Driving range is calculated based on the data: $\frac{\text{Total distance driven}}{\text{Total battery consumed}} \times \text{Battery Size}$.

Table A2: Empirical Test of Range Anxiety

(a) OLS: Dependent variable: log(trip hazard rate)

	(1) Baseline	(2) Morning	(3) Weekend	(4) Winter	(5) Summer
1(Remain. range after a trip <50km)	-0.794***	-0.674***	-0.775***	-0.783***	-0.671***
	(0.158)	(0.197)	(0.112)	(0.130)	(0.181)
1(Remain. range after a trip 50-100km)	-0.229**	-0.163	-0.289***	-0.191***	-0.157
	(0.107)	(0.108)	(0.0973)	(0.0689)	(0.121)
Trip Distance FE	Yes	Yes	Yes	Yes	Yes
R-squared	0.988	0.990	0.979	0.984	0.984

(b) Poisson: Dependent variable: Hazard rate

	(1) Baseline	(2) Morning	(3) Weekend	(4) Winter	(5) Summer
1(Remain. range after a trip <50km)	-0.558***	-0.374**	-0.619***	-0.602***	-0.411***
	(0.132)	(0.166)	(0.0701)	(0.123)	(0.143)
1(Remain. range after a trip 50-100km)	-0.133**	-0.0625	-0.202***	-0.129***	-0.0544
	(0.0619)	(0.0600)	(0.0572)	(0.0414)	(0.0694)
Trip Distance FE	Yes	Yes	Yes	Yes	Yes

Note: The unit of observation is a trip bin, and we categorize all trips into 45 bins based on the starting range and ending range. The table reports the estimated hazard rate drop for trips that end in a low range ($< 50km$ or $50 - 100km$). We control for the trip distance fixed effect.

Table A3: Model Estimates: State Arrival & Transition

	W/out Home Charging		W/ Home Charging	
	Estimate	SE	Estimate	SE
Trip Arrival (per day): peak				
<50km	3.7267	(0.0487)	4.5121	(0.0808)
50-100km	1.5608	(0.0237)	1.5808	(0.0298)
100-150km	0.2438	(0.0068)	0.1546	(0.0045)
150-200km	0.0958	(0.0040)	0.0368	(0.0019)
200-250km	0.0334	(0.0023)	0.0099	(0.0009)
250-300km	0.0155	(0.0018)	0.0034	(0.0006)
300-350km	0.0093	(0.0017)	0.0017	(0.0006)
350-400km	0.0032	(0.0013)	0.0010	(0.0006)
Trip Arrival (per day): off-peak				
<50km	1.4052	(0.0316)	0.8933	(0.0179)
50-100km	0.7494	(0.0193)	0.4199	(0.0095)
100-150km	0.1983	(0.0079)	0.0706	(0.0027)
150-200km	0.0916	(0.0051)	0.0280	(0.0016)
200-250km	0.0459	(0.0035)	0.0103	(0.0010)
250-300km	0.0251	(0.0029)	0.0041	(0.0007)
300-350km	0.0107	(0.0023)	0.0009	(0.0004)
350-400km	0.0058	(0.0022)	0.0003	(0.0004)
Peak Transition				
Pr(OffPeak->Peak)	0.3545	(0.0096)	0.2536	(0.0065)
Pr(Peak->OffPeak)	0.2771	(0.0085)	0.4270	(0.0102)
Location Transition (2021)				
Pr(->CA $\in [0,1]$)	0.4181	(0.0034)	0.5037	(0.0025)
Pr(->CA $\in [1,2]$)	0.3277	(0.0032)	0.3130	(0.0023)
Pr(->CA $\in [2,3]$)	0.1443	(0.0024)	0.1213	(0.0016)
Pr(->Price $\in [0,1.2]$)	0.2498	(0.0030)	0.1994	(0.0020)
Pr(->Price $\in [1.2,1.5]$)	0.1717	(0.0026)	0.1991	(0.0020)
Pr(->Price $\in [1.5,2]$)	0.2969	(0.0031)	0.3865	(0.0024)
Pr(->Amenity $\in [0,1]$)	0.2151	(0.0028)	0.2120	(0.0020)
Pr(->Amenity $\in [1,2]$)	0.2073	(0.0028)	0.2573	(0.0022)
Pr(->Amenity $\in [2,3]$)	0.2550	(0.0030)	0.2668	(0.0022)
Pr(->W/ Private Charger)	0.0000	(NaN)	0.1985	(0.0020)
Location Transition (2024)				
Pr(->CA $\in [0,1]$)	0.1719	(0.0024)	0.2256	(0.0019)
Pr(->CA $\in [1,2]$)	0.0984	(0.0019)	0.1741	(0.0017)
Pr(->CA $\in [2,3]$)	0.2555	(0.0028)	0.2770	(0.0020)
Pr(->Price $\in [0,1.2]$)	0.2887	(0.0029)	0.2027	(0.0018)
Pr(->Price $\in [1.2,1.5]$)	0.1849	(0.0025)	0.2276	(0.0019)
Pr(->Price $\in [1.5,2]$)	0.2700	(0.0028)	0.3670	(0.0021)
Pr(->Amenity $\in [0,1]$)	0.2251	(0.0027)	0.2667	(0.0020)
Pr(->Amenity $\in [1,2]$)	0.2302	(0.0027)	0.2826	(0.0020)
Pr(->Amenity $\in [2,3]$)	0.2683	(0.0028)	0.2392	(0.0019)
Pr(->W/ Private Charger)	0.0000	(NaN)	0.2108	(0.0018)

Notes: The Number of observations is 8000 drivers with 214,000 sessions. The table reports estimated Poisson trip arrival rates and transition probabilities by types (with or without home chargers, under the 2021 or 2024 network).